

## FLUID CIRCULATION AND FAULT- AND FRACTURE-RELATED DIAGENESIS IN MISSISSIPPIAN SYN-RIFT CARBONATE ROCKS ON THE NORTHEAST MARGIN OF THE METALLIFEROUS DUBLIN BASIN, IRELAND

KEVIN L. SHELTON,<sup>1</sup> JAMES P. HENDRY,<sup>2</sup> JAY M. GREGG,<sup>3</sup> JON P. TRUESDALE,<sup>1</sup> AND IAN D. SOMERVILLE<sup>4</sup>

<sup>1</sup>Department of Geological Sciences, University of Missouri, Columbia, Missouri 65211, U.S.A.

<sup>2</sup>Tullow Oil Limited, Number 1 Central Park, Leopardstown, Dublin 18, Ireland

<sup>3</sup>Boone Pickens School of Geology, Oklahoma State University, Stillwater, Oklahoma 74074, U.S.A.

<sup>4</sup>School of Earth Sciences, University College Dublin, Belfield, Dublin 4, Ireland

e-mail: [jim.hendry@tullowoil.com](mailto:jim.hendry@tullowoil.com)

**ABSTRACT:** Lower Carboniferous (Mississippian) limestones exposed on the northeastern margin of the Dublin Basin comprise syn-rift, shallow marine carbonate platform, and deep-water carbonate turbidite sequences. Multiple generations of fault- and fracture-related carbonate and quartz veins cut the strata and are locally associated with massive dolomitization of adjacent limestones. Associated saddle dolomite cements display inconsistent cathodoluminescence stratigraphies despite a common paragenetic context. Fluid inclusions record interaction of two end-member paleofluids: a moderate- to high-temperature ( $T_h \sim 150$  to  $300^\circ\text{C}$ ), low- to moderate-salinity brine, and a low-temperature ( $T_h \sim 60$  to  $135^\circ\text{C}$ ), high-salinity brine. Isotope analyses of host limestone, dolomite, and carbonate veins define trends of  $\delta^{18}\text{O}$  values from  $\sim -3$  to  $-22\text{‰}$  VPDB,  $\delta^{13}\text{C}$  values from  $+4$  to  $-4\text{‰}$  VPDB, and  $^{87}\text{Sr}/^{86}\text{Sr}$  values from 0.7080 to 0.7105. The wide ranges in  $\delta^{18}\text{O}$  and  $^{87}\text{Sr}/^{86}\text{Sr}$  values of calcite veins reflect incursion of highly evolved waters that interacted to varying degrees with more radiogenic rocks along their flow paths and with the host limestones into which they were emplaced. Field evidence, including orientations of vein- and dolomite-associated faults, and presence of reworked zebra dolomites in Brigantian hanging wall debris-flow conglomerates, support a Viséan age of mineralization. Comparison with published data from the Irish Midlands and central Dublin Basin supports a conceptual model of syn-rift fluid flow where regional saline paleoaquifers were intercepted by localized hydrothermal cells on active faults, some of which extended into lower Paleozoic basement. Episodes of structurally controlled hydrothermal fluid flow, cooling and mixing of fluids, and variable fluid–rock interaction led to a suite of similar diagenetic products but a diversity of compositions that are neither geographically nor stratigraphically correlated. This study presents a rare example of syn-rift diagenesis recorded in syn-rift limestones on the margins of a metalliferous basin.

### INTRODUCTION

Major economic Pb–Zn–sulfide deposits with associated dolomite and calcite gangue mineralization have been described across the Irish Midlands (e.g., Lisheen in the Rathdowney Trend), as well as key sites in the northern Dublin Basin (e.g., Navan). A consensus is that diagenetic mineralization occurred during shallow burial and involved interaction of multiple fluid types (e.g., Wright et al. 2000; Gregg et al. 2001; Johnson et al. 2009; Wilkinson 2010). In particular, two dominant fluids have been documented: fault-controlled, higher-temperature–lower-salinity fluids related to rifting (Wilkinson and Earls 2000; Banks et al. 2002; Wilkinson 2003, 2010) and regionally extensive, lower-temperature–higher-salinity brines (Johnston 1999; Wright et al. 2000; Gregg et al. 2001; Johnson et al. 2009). Various hydrological models for mineralization have invoked deep convection cells scavenging base metals from basement rocks (Russell 1978, 1986), gravity-driven basinal brines (Hitzman and Beaty 1996; Hitzman et al. 1998), and hybrid models of basement-involved metalliferous brines mixing with sulfide-bearing brines (see Wilkinson and Hitzman 2015 for a review).

We extend these studies to deformed Mississippian platform carbonates and carbonate turbidites exposed along the northeastern Irish coast at Howth, Loughshinny, and Malahide (Fig. 1A, B), where multiple generations of fault- and fracture-related quartz and carbonate veins are locally associated with massive dolomitization of adjacent limestones. The succession is important in recording a syn-rift basin to platform-top succession through the Tournaisian and Viséan on the margin of the Dublin Basin (Fig. 2). It therefore provides an opportunity to test the syn-rift model for Irish mineralization in a demonstrably syn-rift succession. This provides further insight into the Dublin Basin system, with additional relevance to generic models of fluid expulsion from hanging-wall basins onto footwall carbonate platforms, and on fault-controlled fluid flow and carbonate mineralization in extensional basins (e.g., Keller et al. 2000; Davies and Smith 2006; López-Horgue et al. 2010; Martín-Martín et al. 2015; Hollis et al. 2017). It also provides a data set comparable to other published studies of the diagenetic and mineralization history of Mississippian limestones in the NW British Isles, specifically the North Wales, Derbyshire, and Isle of Man platforms, where discrepancies exist

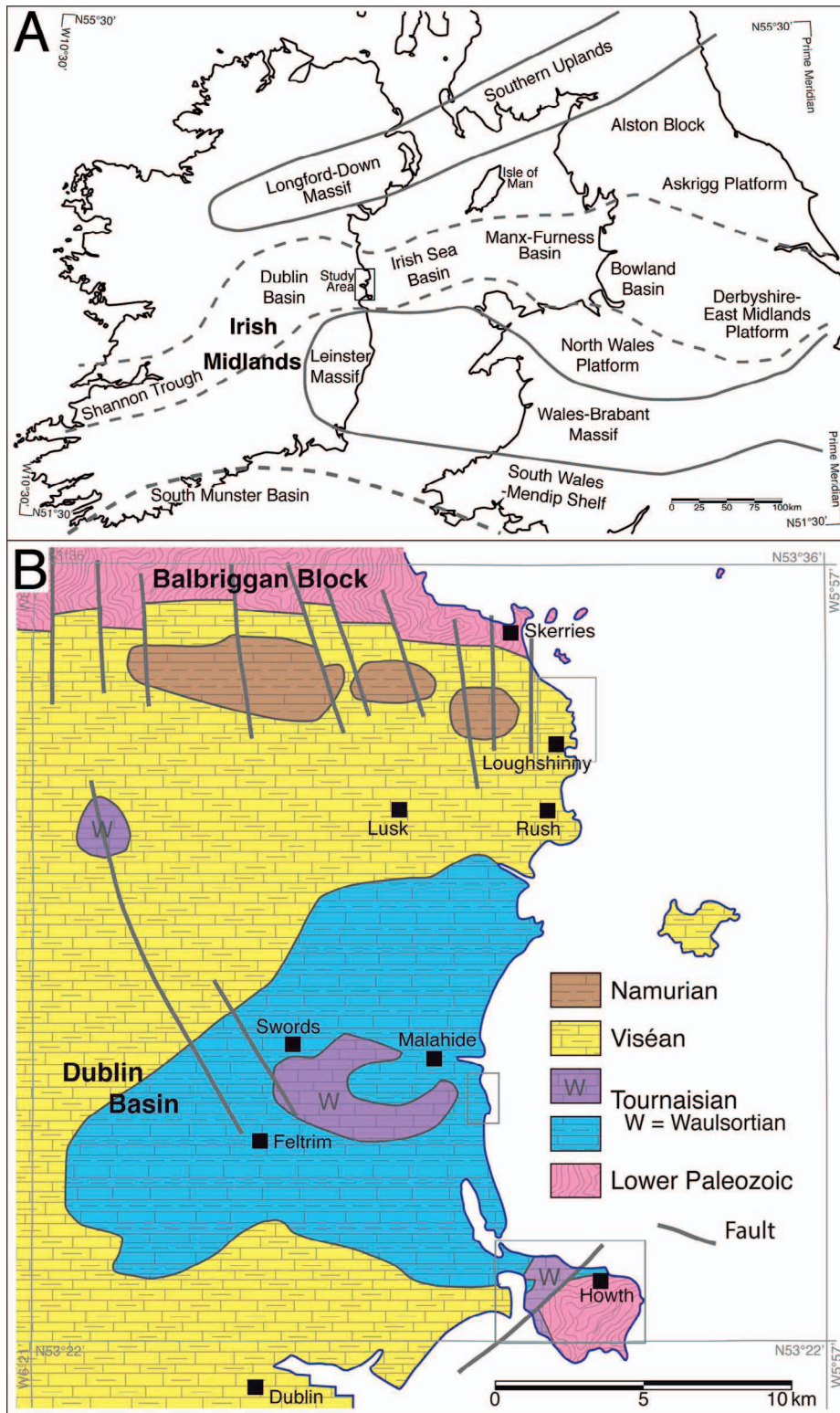


FIG. 1.—**A**) Regional map showing location of study area (rectangular box) relative to basins, platforms, and massifs (modified after Juerges et al. 2016). **B**) Simplified geological map of the eastern part of the Dublin Basin (after Somerville et al. 1992a). Boxes outline the three localities of this study.

with respect to timing, tectonic context, and origins of diagenetic fluids (e.g., Frazer et al. 2014, and references therein; Hendry et al. 2015; Juerges et al. 2016).

Several specific questions regarding the northeast margin of the Dublin Basin are posed: (1) What control do stratigraphy and facies exert on the diagenesis and fluid history of basinal and shelf carbonates along the basin

margin? (2) Are carbonate and quartz veins in syn-rift strata part of a regional paleohydrological system, or do they represent discrete fault-related flow systems? (3) What roles do tectonics and basement lithology play in whether vein-related fluids also deposited Cu- or Pb-Zn mineralization, or no ores at all? These questions are addressed by combining petrographic, fluid-inclusion, and isotopic (C, O, and Sr)

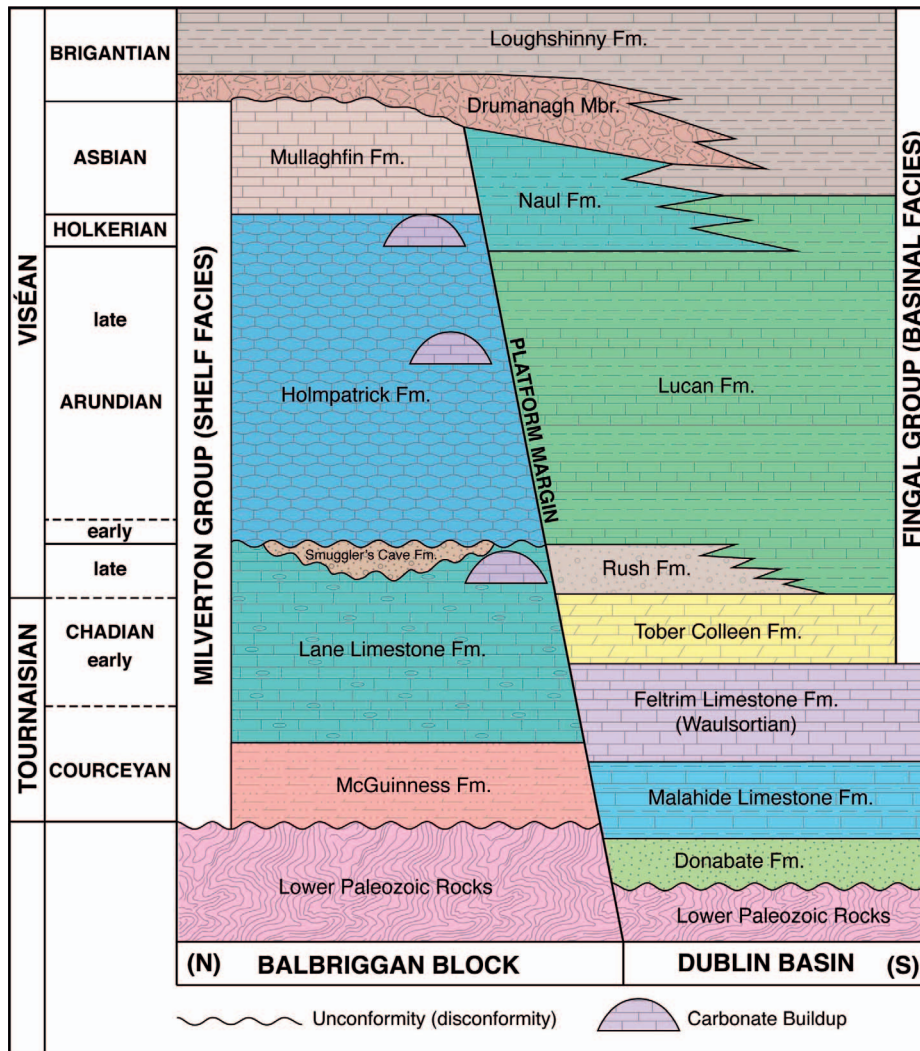


FIG. 2.—Generalized Lower Carboniferous stratigraphy and lithologies of the eastern edge of the Dublin Basin (after Strogon et al. 1990; Somerville et al. 1992a). Basinal sedimentary rocks of the Fingal Group are about twice as thick ( $\geq 1500$  m) as coeval shelf deposits of the Milverton Group (Pickard et al. 1994).

analysis of carbonate-hosted quartz, dolomite, and calcite veins and their respective host rocks.

#### REGIONAL AND LOCAL GEOLOGY OF THE NORTHEAST DUBLIN BASIN

The Dublin Basin (Fig. 1A) is an intracratonic extensional basin that for long periods behaved as a linear, E–W-trending depocenter. Shallow-water platform areas on the north and south margins, adjacent to the Balbriggan Block and Leinster Massif (Fig. 1B), were present throughout the Viséan with synchronous deposition of deep- and shallow-water carbonate facies (Somerville et al. 1992a). The stratigraphy, facies, and thickness variations in the basin have been extensively described (MacDermot and Sevastopulo 1972; Nolan 1986, 1989; Rees 1987; Jones et al. 1988; Somerville et al. 1992a, 1992b; Philcox et al. 1995; Strogon et al. 1990, 1996; Sevastopulo and Wyse Jackson 2009; Somerville and Waters 2011). The lithostratigraphy of the basin can be divided into a lower continental red-bed sandstone, a thick sequence of syn-rift marine carbonate rocks, comprising the Tournaisian and Viséan series of the Lower Carboniferous (Mississippian), and overlying Namurian (Pennsylvanian) marine and nonmarine siliciclastic rocks (Fig. 2) (Wright et al. 2003). Sedimentation in the late Tournaisian was initially on a ramp, but early rifting commencing in the late Chadian transformed this into discrete fault blocks with shallow-marine carbonates deposited on the footwalls (e.g., Balbriggan Block, Fig. 2) and rapidly subsiding hanging-wall basins. These accumulated deep-

water carbonates and shales, and gravity-flow deposits of shallow-water carbonates reworked from the adjacent platforms during renewed active rifting in the early Brigantian (Pickard et al. 1994; Strogon et al. 1996). Rifting was widespread across the British Isles in the early and late Viséan (Gawthorpe et al. 1988) and was associated with back-arc extension to the north of the Variscan orogenic front (Smit et al. 2018). During the Late Carboniferous Variscan orogeny the northeast Dublin Basin was inverted, with renewed rifting and subsidence in the early Mesozoic like that in adjacent offshore Irish Sea basins (Newman 1999).

Mississippian carbonate rocks are the host for Zn and Pb sulfide deposits in the Dublin Basin and Irish Midlands (Braithwaite and Rizzi 1997; Wilkinson and Hitzman 2015). Areas near Dublin (Figs. 1B, 3–7) are characterized by ENE–WSW-trending normal faults showing NE–SW extension (Wright et al. 2000), although some E–W- and N–S-trending faults are locally present. Similar fault and vein orientations are recorded from the adjacent Irish Midlands (de Brit 1989).

#### Tournaisian Strata

Tournaisian limestones exposed on the north Dublin coast are among the oldest Lower Carboniferous rocks in the Dublin Basin (Jones et al. 1988; Somerville and Waters 2011). They comprise folded and faulted blocks of the Malahide Limestone, Feltrim Limestone, and Tober Colleen formations (Fig. 2). Steeply dipping Viséan faults, reactivated in the Variscan orogeny,

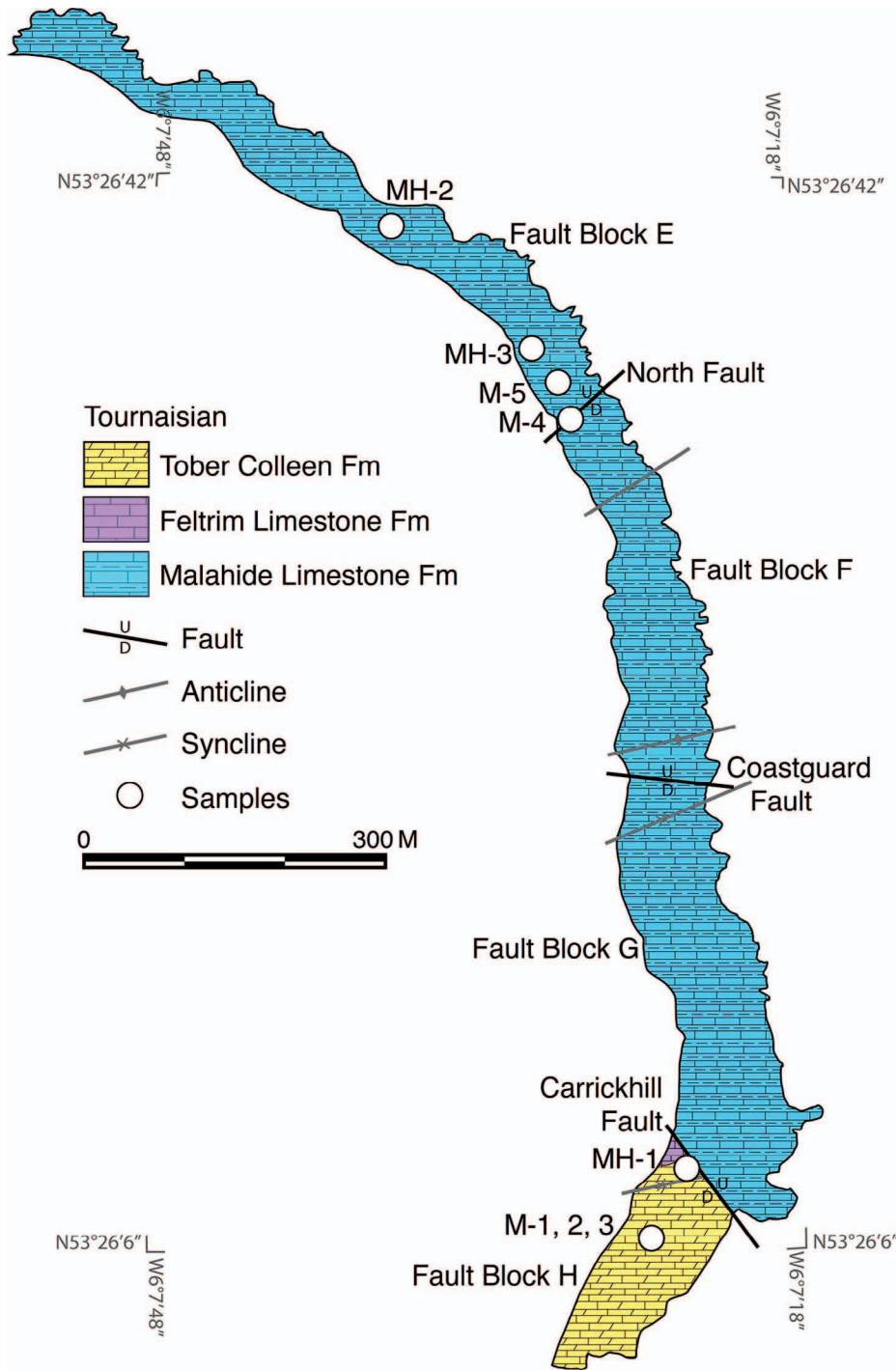
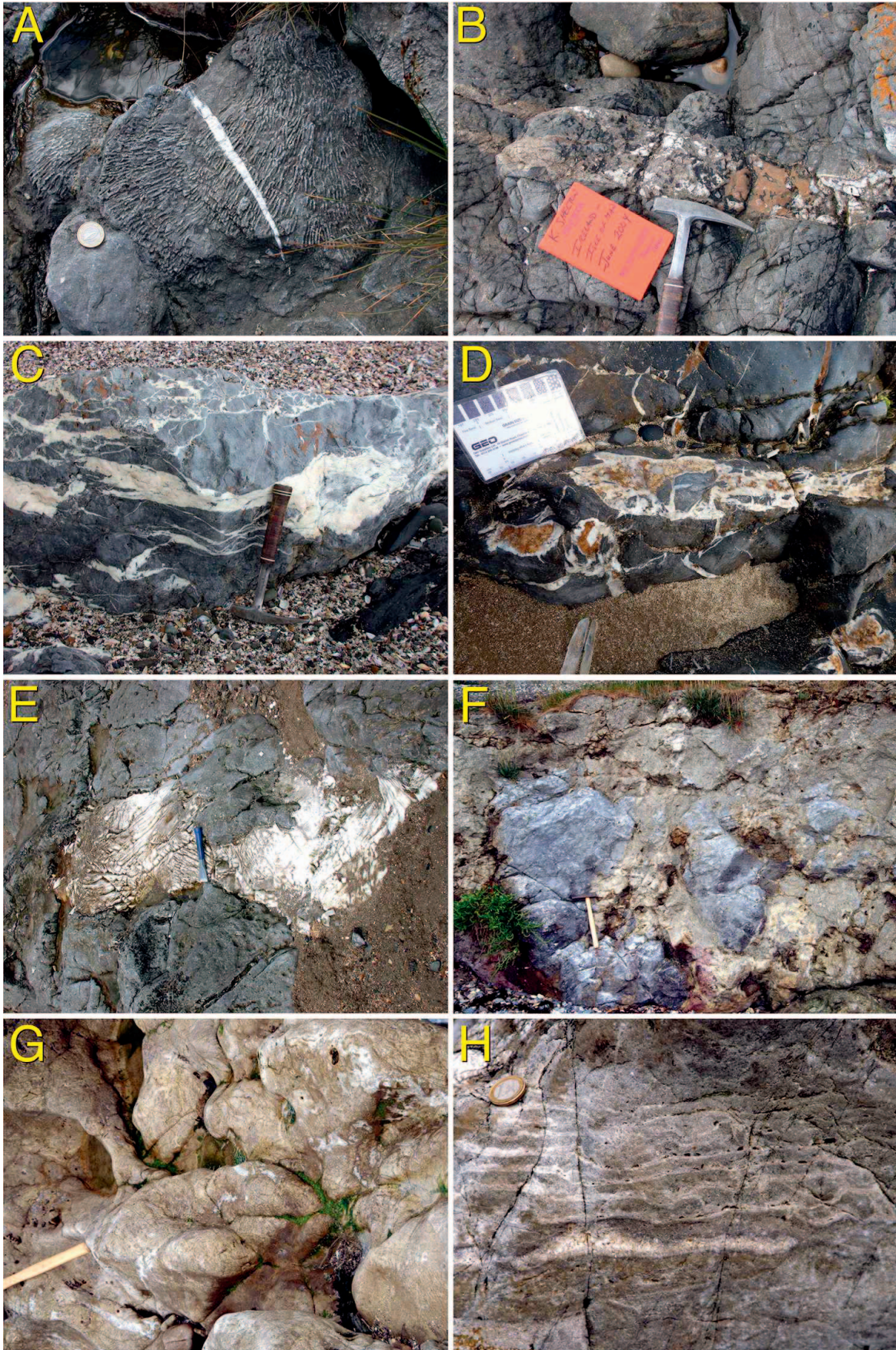


FIG. 3.—Geological map of the Malahide coastal area with sample localities in Tournaisian basinal limestones (after Philcox et al. 1995). Samples MH 1–3 were collected and reported in Wright (2001).

FIG. 4.—Images of Tournaisian strata exposed on the north Dublin coast. A–D) Malahide. A) Fibrous white calcite vein crosscutting overturned tabulate coral (*Syringopora*) of the Malahide Formation (coin is ~ 2.5 cm). B) Brown dolomite vein cutting gray Malahide Formation limestone (hammer's head is 18 cm long). C) Anastomosing calcite veins crosscutting Tober Colleen Formation (hammer is 33 cm long). D) Saddle dolomite–calcite vein in the Tober Colleen Formation limestone (scale card is 10 cm wide). E–H) Howth outcrops of the Feltrim Formation. E) Large calcite vein in grey limestone along Claremont Strand (chisel is 20 cm long). F–H) Outcrops near Sutton Dinghy Club: F) Gray limestone blocks in brown dolomitized matrix (hammer is 40 cm long). G) Tan dolomite containing calcite veins (hammer handle is 35 cm long). H) Zebra dolomite consisting of layers of dolomitized host rock interspaced with sheet pores lined by saddle-dolomite cement (coin is ~ 2.5 cm).



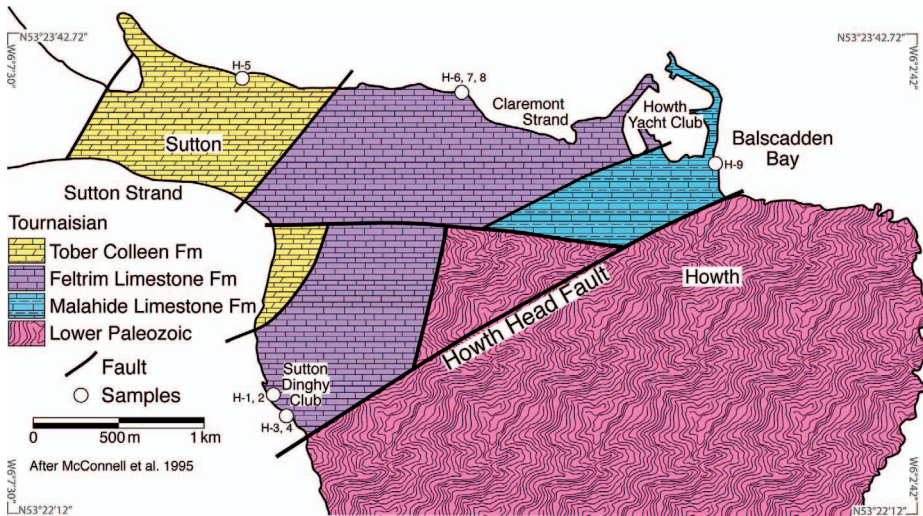


FIG. 5.—Geologic map of Howth coastal area with sample locations in Tournaisian basinal limestones (after Somerville et al. 1992a; McConnell et al. 1995).

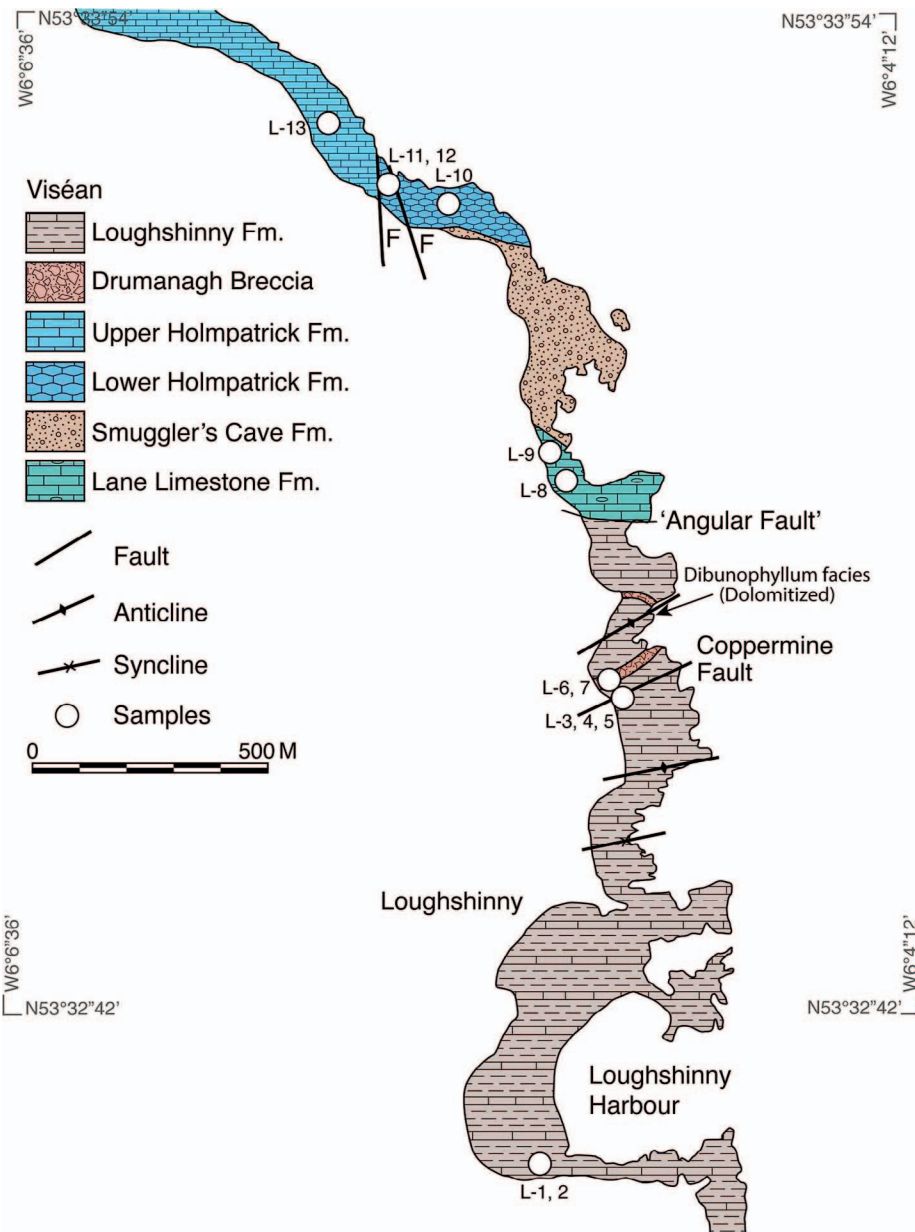


FIG. 6.—Geological map of the Loughshinny coastal area with sample localities (after Philcox et al. 1995). Traditionally, the contact between the Lane and Loughshinny formations was called an “angular fault,” though it is an angular unconformity. However, at depth, the southern margin of the Balbriggan shelf block was most likely a normal (extensional) fault.

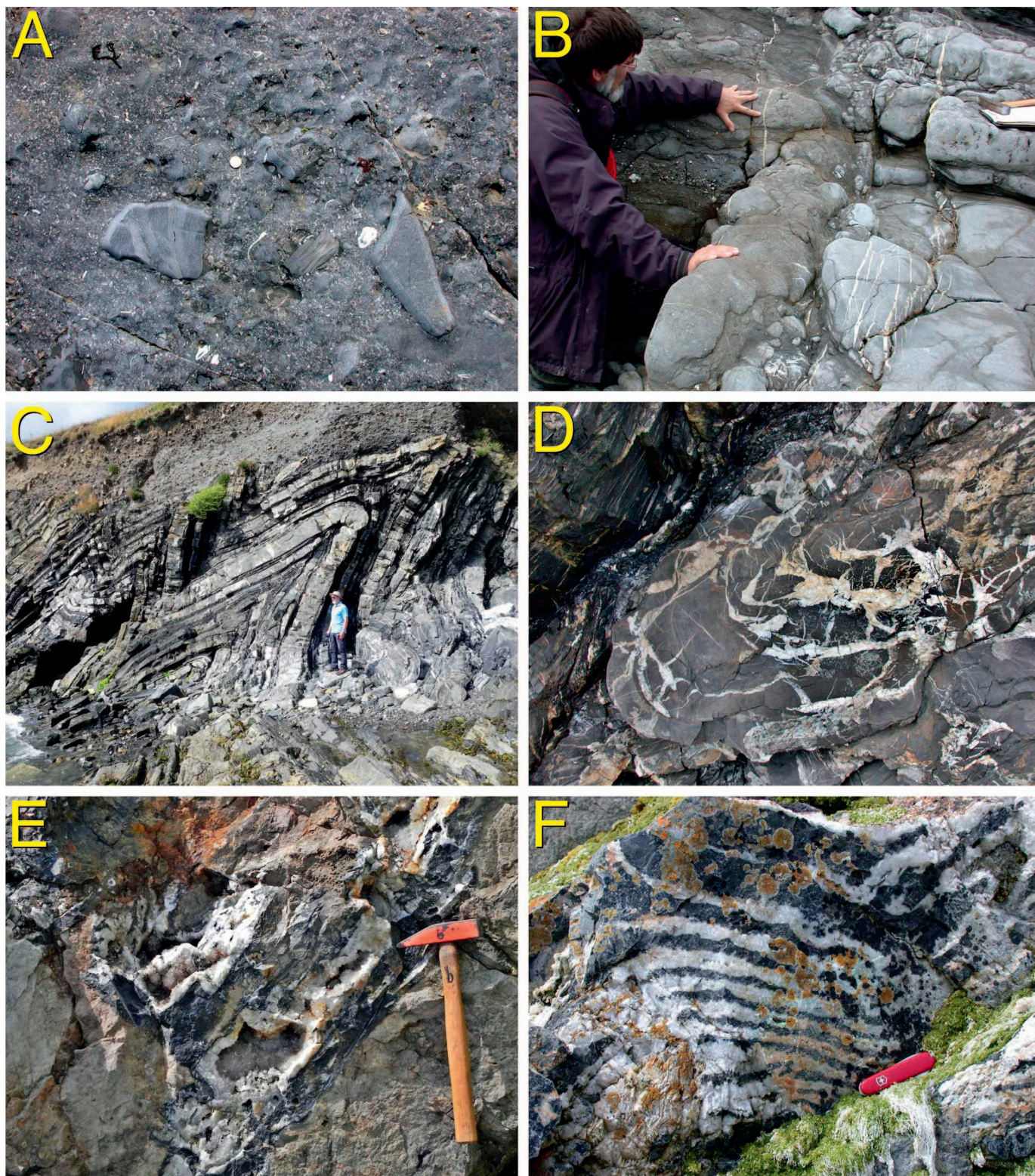


FIG. 7.—Images of Viséan strata exposed at Loughshinny. **A)** Limestone clasts and fossil fragments in debris-flow breccia in the Drumanagh Member of the Loughshinny Formation (coin is  $\sim 2.5$  cm). **B)** Calcite veins ( $\sim 0.5$  cm wide) cutting the debris flow. **C)** Chevron folds in carbonate turbidites of the Loughshinny Formation (person for scale,  $\sim 175$  cm tall). **D)** Folded veins in the nose of a syncline of the Loughshinny Formation (coin is  $\sim 2.5$  cm). **E)** Chalcedonic to coarse-grained quartz veins at Coppermine Fault (hammer is 40 cm long). **F)** Zebra texture (brown dolomite and white quartz) of the Loughshinny Formation adjacent to quartz veins shown in Part E (knife is  $\sim 8$  cm long).

divided the section into several distinct fault blocks (Matley and Vaughan 1908; Marchant 1978; Philcox et al. 1995). Throw on individual faults is difficult to estimate on the foreshore exposures because of limited outcrop and subsurface data, but is likely to be several hundreds of meters (e.g., Carrickhill Fault) (Fig. 3).

The Malahide Limestone Formation is exposed on the foreshore at Malahide in three fault-bounded blocks (E, F, and G, Fig. 3). Strata in the northernmost Block E dip from 35° N near the NE-striking North Fault to 10° N away from the fault, and consist of dark gray wackestones, packstones, and grainstones with abundant tabulate corals (*Syringopora*) (Philcox et al. 1995) (Fig. 4A). Strata adjacent to and for about 10 m north of the fault are comprised of extensively dolomitized grainstones and packstones that weather brown and have a distinct sucrosic texture (Fig. 4B). Dolomite–limestone contacts are millimeter-sharp to slightly diffuse (a few centimeters wide); they can follow bed boundaries but commonly cut across bedding, and “tongues” of dolomite can be seen to extend preferentially along thick beds of cross-bedded grainstone. Blocks F and G consist of decimeter-scale, shallowing-upward cycles with laminated argillaceous mudstones overlain by nodular, bioturbated, richly fossiliferous packstones and grainstones, and capped by low-angle-cross-bedded crinoidal grainstones and rudstones. The last are commonly dolomitized adjacent to faults, and dolomite locally extends into other facies. The southernmost Block H contains deeper-water (basinal) facies (Somerville et al. 1992b; Somerville 2003), including massive pale gray limestones of the Feltrim Limestone Formation (Waulsortian mud mound facies) and darker gray limestone–shale beds of the Tober Colleen Formation. The latter is dominant, comprising nodular to thin-bedded, argillaceous and sparsely fossiliferous silty mudstones, wackestones, and calcareous shales with sporadic debris deposits of grainstones and poorly sorted pebble- to boulder-size clasts sourced from the Feltrim Limestone. Abundant centimeter-thick dolomite–calcite veins extend towards the northern margin of Block H and are parallel to and likely associated with the adjacent NW-striking Carrickhill Fault (Philcox et al. 1995) (Fig. 4C, D).

At Howth, the same formations are separated from adjacent basement rocks by a large NE–SW, steeply NW dipping normal fault (Fig. 5) (the “Howth Head Fault,” HHF). This is characterized by a  $\geq 2$ -m-thick, iron- and manganese-oxide-cemented footwall breccia and based on local stratigraphic relationships has a likely minimum throw of  $> 55$  m. The basement rocks consist of lower Paleozoic quartzite, phyllite, and graywacke cut by quartz veins, which are thought to be associated with the Caledonian orogeny (O’Hara 1995). Here the Feltrim Limestone Formation consists of fine-grained, pale to medium gray, massive mud-mound biohermal limestones (Waulsortian “reef”) with few fossils cut by variably oriented large veins of coarse calcite (Fig. 4D). On the west side of the Howth peninsula (near the Sutton Dinghy Club), for  $\sim 300$  m west of the fault, much of the Waulsortian facies exposed on the foreshore has been partially replaced by pale brown dolomite (Fig. 4E) and commonly contains irregular to sheet-like, centimeter-size vugs filled with white calcite (Fig. 4F). A meter-scale exposure of zebra dolomite texture (cf. Vandeginste et al. 2005), consisting of layers of dolomitized host rock interspaced with sheet pores lined with saddle dolomite cement, is also present (Fig. 4G). Some of these dolomitized rocks have been crosscut by later calcite veins (Fig. 4F).

### Viséan Strata

The Loughshinny area has been interpreted as comprising the hanging-wall blocks of progressively imbricated basement-rifted structures that formed in two stages, the first in the Chadian and the second from the Asbian to the Brigantian (Nolan 1989; Harrison and Henderson 2004). The Loughshinny Block (Fig. 6) is fault-bounded to the north and contains the youngest Carboniferous rocks investigated. The Loughshinny Formation

(Brigantian) consists of dark gray intercalated, graded and sharp-based packstones–wackestones, argillaceous and/or cherty mudstones, and calcareous shales. It is interpreted as the syn-rift part of the deep-marine North Dublin Basin succession. The uplifted Balbriggan Block hosts pale to medium gray bioclastic grainstones, packstones, and shaly nodular wackestones, calcareous sandstones, and pebble beds of the Lane and Holmpatrick formations, reflecting shallow marine deposition on the North Dublin Shelf (Figs. 2, 6, 7). The limestones contain a diverse fauna, including brachiopods, crinoids, foraminifers, ostracods, solitary corals, and less commonly, trilobites. These formations are separated by a gray coarse siliciclastic breccio-conglomerate, the Smuggler’s Cave Formation, which overlies a late Chadian karstic surface and paleosol capping the Lane Limestone and has been interpreted as a fluvial deposit (Nolan 1986, 1989).

Sequences and structures exposed on the coast from south to north are distal calciturbidites of the Loughshinny Formation; the NE-trending Coppermine Fault; the NE-trending Popeshall anticline, comprising the polymict Drumanagh Member breccia/conglomerate (also called the Popeshall boulder bed) that overlies dolomitized *Dibunophyllum* coral-containing limestone in the core of the fold; the Lane Limestone; the Smuggler’s Cave Conglomerate; and the Holmpatrick Formation (Nolan 1986, 1989; Philcox et al. 1995; Somerville and Waters 2011). The Drumanagh Member is thick-bedded conglomeratic debris-flow deposit, with abundant crinoids and brachiopods and subangular to subrounded, centimeter–decimeter size clasts of dark to pale bioclastic limestone, dolomite, and vein quartz (Fig. 7A, B). This and the Smuggler’s Cave Conglomerate are interpreted as having been reworked from the Balbriggan Block during Chadian and Asbian to Brigantian events, respectively (Nolan 1989; Pickard et al. 1994; Harrison and Henderson 2004).

The Loughshinny Formation was deformed during the Variscan orogeny into a series of chevron folds at Loughshinny Harbour at the southern end of the study area. At least three generations of crosscutting fracture and vein sets with calcite and minor quartz cement occur in the deformed carbonate turbidites (Fig. 7C, D). In fold hinge zones the limestones are variably recrystallized to anhedral calcite spar mosaics showing abundant deformation twins. Vein orientations are complex; the earliest calcite veins are subparallel to and folded with the host strata, and two later sets of crosscutting fractures. Along the damage zone of the ENE-striking, steeply S-dipping Coppermine Fault to the north, meter-scale quartz veins with dolomite selvages and decimeter-size veins and vugs contain rims of chalcopyrite, malachite, and azurite that were mined during the nineteenth century near Popeshall. Open-space-filling quartz and later dolomite cement are associated with the copper-sulfide mineralization. Silicified zebra fabrics and vug-lining quartz cements are also present immediately adjacent to the fault (Fig. 7E, F). North of the fault for 200 m, Loughshinny Formation limestones are partly to completely replaced by pale brown dolomite and contain frequent irregular millimeter–centimeter vugs, sheet vugs, and zebra fabrics filled by coarse white saddle dolomite. Some dolomite clasts in the Drumanagh Member are also characterized by zebra sheet pores lined by saddle dolomite cement (Fig. 8A). Dolomite–limestone boundaries are millimeter-sharp and cut across stratification (Fig. 8B). Multiple generations of millimeter–centimeter, gray to brown calcite veins cut both limestone and dolomite host rocks in various orientations, and they locally occur at the dolomite–limestone contacts.

Faults in the Holmpatrick Formation are associated with a variety of veins and bodies of pervasively dolomitized limestone associated with the faulting. White, gray and yellow-brown calcite veins subparallel to N- and NNW-striking faults cut the dolomitized limestones and locally occur at the dolomite–limestone contacts, and rare white quartz veins are also present close to the faults.



FIG. 8.—Images of Viséan strata exposed at Loughshinny. **A**) Rounded clast of dolomite containing zebra sheet pores lined by saddle dolomite in a debris flow of the Drumanagh Breccia, indicating that some dolomite had formed at sufficiently shallow depths to be reworked before debris-flow emplacement (coin is  $\sim 2.5$  cm). **B**) Sharp contact between limestone (gray) and dolomite (brown) with cemented vugs close to a fault in the Holmpatrick Formation (scale card, arrowed, is 10 cm wide).

#### SAMPLING AND METHODS

Sixty-two specimens were collected, and their positions were recorded by GPS and plotted onto Google Earth imagery (Table 1). Field photographs were similarly indexed using GPS coordinates. Rock specimens were sawn and prepared for petrographic examination as highly polished thin sections made from freshly cut surfaces. They were examined by conventional optical microscopy and in cathodoluminescence (CL) utilizing a CITL CL8200 MK5 cold cathode optical CL system. Selected cut surfaces and thin-section billets were stained with Alizarin Red S and potassium ferricyanide for discrimination of dolomite and calcite (Dickson 1965).

Fluid-inclusion microthermometry was performed on doubly polished wafers made from selected specimens of dolomite, calcite, and quartz, taking care to analyze primary or pseudosecondary inclusions based on shape, distribution within crystals, and consistent size and vapor:liquid ratios (Roedder 1984; Goldstein and Reynolds 1994). Microthermometric data were obtained using a USGS-type gas-flow heating/freezing stage (Table 2). Temperatures of total homogenization ( $T_h$ ) have errors of  $< \pm 2^\circ\text{C}$ , and temperatures of melting ( $T_m$  of ice and clathrate) have errors of  $< \pm 0.2^\circ\text{C}$ , based on replicate measurements of standard fluid inclusions (Shelton and Orville 1980). Compositions of the trapped fluids were determined from thermometric data using MacFlinCor software (Brown

and Hagemann 1995) and data of Bodnar (1993) and Bodnar and Vityk (1994). No pressure corrections were made to  $T_h$  data.

Sixty-two samples were micro-drilled from thin-section billets under a binocular microscope for stable-isotope analysis (Table 3). Carbon and oxygen isotope compositions of carbonates were determined using a Thermo-Finnigan Delta Plus gas-source mass spectrometer with a Kiel device at the University of Missouri. The  $\delta^{13}\text{C}$  and  $\delta^{18}\text{O}$  values are reported relative to VPDB with standard errors of  $< \pm 0.05\%$  ( $2\sigma$ ) based on replicate analyses of NBS-19 calcite, and dolomites have been corrected for reaction with 103% phosphoric acid at  $50^\circ\text{C}$  (Rosenbaum and Sheppard 1986). Two slightly dolomitized limestones were considered as calcites, as no attempt at mineralogical separation was made. Two dolomite samples from the Malahide Formation analyzed by Wright (2001) are incorporated into the data set. Quartz was reacted with  $\text{ClF}_3$  using a modification of the Clayton and Mayeda (1963) method. Precision for  $\delta^{18}\text{O}$  analyses of quartz samples (VSMOW) was  $< \pm 0.20\%$ . Splits from twenty of the carbonate sample powders were analyzed for strontium-isotope composition using conventional preparation techniques and thermal ionization mass spectrometry (TIMS) at the University of Kansas. Analytical precision was monitored by repeated analysis of NBS-987 and is better than  $\pm 0.000014$  at the 95% confidence interval. All measured  $^{87}\text{Sr}/^{86}\text{Sr}$  data have been normalized to the NBS-987 literature value of 0.710248 (McArthur et al. 2000). Precision of Sr concentration analysis is better than  $\pm 10$  ppm.

TABLE 1.—North Dublin coast sample localities and descriptions.

Locality	Latitude, Longitude	Location	Formation	Description
<b>Tournaisian Howth</b>				
H-1	53°22'36"N, 6°6'7"W	Sutton Dinghy Club	Feltrim	brown dolomitized limestone with vuggy white calcite vein
H-2	53°22'31"N, 6°6'6"W	40 m NW of H-1	Feltrim	brown dolomitized limestone cut by gray calcite vein
H-3	53°22'81"N, 6°6'1"W	100 m SE of Dinghy Club	Feltrim	brown zebra dolomite in limestone
H-4	53°22'32"N, 6°6'3"W	40 m SE of H-4	Feltrim	bedded dolomite with vug-filling calcite (315–320° strike, 26° NE dip)
H-5	53°23'34"N, 6°6'15"W	Claremont Strand	Feltrim	partially dolomitized limestone cut by white calcite vein
H-6	53°23'32"N, 6°5'6"W	below Howth Lodge	Feltrim	dolomite + calcite vein in limestone
H-7	53°23'32"N, 6°5'6"W	below Howth Lodge	Feltrim	30-cm-wide calcite vein in limestone (280° strike, 90° dip)
H-8	53°23'32"N, 6°5'6"W	below Howth Lodge	Feltrim	vug-filling dolomite and gray calcite vein cutting limestone
H-9	53°23'19"N, 6°3'48"W	Balscadden Bay	Malahide	calcite vein in limestone (035° strike, 88° SE dip)
<b>Malahide</b>				
MH-1	53°26'9"N, 6°7'18"W	Fault Block H, near Carrickhill Fault	Tober Colleen	argillaceous fine crystalline limestone
MH-2	53°26'40"N, 6°7'35"W	1st debris bed in Fault Block E	Malahide	calcite veins in limestone
MH-3	53°26'36"N, 6°7'27"W	Waulsortian block above upper debris bed, Block E	Malahide	calcite veins in limestone
M-1	53°26'6"N, 6°7'20"W	Fault Block H, near Carrickhill Fault	Tober Colleen	white calcite vein cutting limestone
M-2	53°26'6"N, 6°7'20"W	Fault Block E	Malahide	en echelon calcite veins in limestone (037° strike, 88°SE dip)
M-3	53°26'6"N, 6°7'20"W	Fault Block E	Malahide	brown-gray calcite vein cutting limestone (003° strike, 90° dip)
M-4	53°26'33"N, 6°7'25"W	Fault Block E	Malahide	calcite veins at North Fault
M-5	53°26'35"N, 6°7'26"W	Fault Block E	Malahide	Malahide Limestone a few meters north of North Fault, dolomitized grainstone
<b>Viséan Loughshinny</b>				
L-1	53°32'31"N, 6°4'58"W	Loughshinny Harbour	Loughshinny	multiple calcite vein sets in folded calciturbidite; early set is folded (280° axis); later sets crosscut early veins
L-2	53°32'31"N, 6°4'58"W	Loughshinny Harbour	Loughshinny	large, late-generation calcite vein in calciturbidite
L-3 & 5	53°33'3"N, 6°4'46"W	Coppermine Fault	Loughshinny	m-scale banded quartz vein (275° strike, 41°S dip); chalcidonic quartz overgrown by clear cm-scale quartz
L-4	53°33'3"N, 6°4'46"W	Coppermine Fault	Loughshinny	dolomitized limestone adjacent to quartz vein
L-6	53°33'5"N, 6°4'49"W	N of Coppermine Fault	Loughshinny	dolomite crystals on quartz in zebra dolomite
L-7	53°33'5"N, 6°4'49"W	10 m N of L-6	Loughshinny	dolomite vein cutting dolomitized debrite breccia
Drumanagh Member				
L-8	53°33'19"N, 6°4'53"W	N of Angular Fault	Lane	en echelon calcite veins in limestone (356–004° strike, 90° dip)
L-9	53°33'21"N, 6°4'55"W	South of Smuggler's Cave	Lane	fibrous yellow calcite vein in limestone
L-10	53°33'39"N, 6°5'8"W	faulted Holmpatrick Fm.	Holmpatrick	massive white quartz vein cutting grainy limestone
L-11	53°33'41"N, 6°5'15"W	Near north trending faults	Holmpatrick	dolomitized limestone (semi-zebra fabric)
L-12	53°33'41"N, 6°5'15"W	20 m N of L-11	Holmpatrick	fibrous calcite vein cutting limestone
L-13	53°33'45"N, 6°5'23"W	200 m NW of L-11	Holmpatrick	calcite veins in limestone (312° strike, 90° dip)

#### PETROGRAPHY

The diagenesis and dolomitization of Lower Carboniferous strata in the Dublin Basin have previously been described in detail by Lees and Miller (1995), Gregg et al. (2001), Wright et al. (2003, 2004), and Nagy et al. (2004, 2005a, 2005b), amongst others. The focus of the current study is on interpretation of fault- and fracture-related quartz and carbonate veins and their relationship with associated dolomites. Petrographic descriptions are summarized below and in Figures 9 through 11 to provide a paragenetic framework and context (Fig. 12) for this interpretation. There is much similarity between the sampled Tournaisian and Viséan strata in terms of widespread and volumetrically significant diagenetic products (i.e., excluding localized or minor symsedimentary precipitates).

The first postdepositional diagenetic process recorded in the strata is cementation by turbid, dull-CL, isopachous cryptofibrous calcite, which is restricted to mud-mound biohermal facies of the Feltrim Formation, where it typically lines stromatolite cavities (Fig. 9A). Its characteristics are typical of a marine, near-surface precipitate. In bioclastic grainstones of the Viséan Lane Formation, finely crystalline (0.01–0.1 mm) calcite spar lines primary porosity, and coarser anhedral spar forms epitaxial overgrowths on crinoids. Both are dull brown in CL and are likely to have formed during very early burial from marine pore fluids. These marine cements are overgrown by localized fine-medium crystalline (0.1–0.25 mm), bright

yellow to dull brown CL blocky calcite spar, which coarsens to dark brown CL equant spar in pore centers (Fig. 9C, D). In the absence of evidence for subaerial emergence, vadose fabrics, or complex CL zoning, these cements are assumed to have formed during burial in the original marine pore fluids. Blocky calcite is the dominant cement in limestones of the Feltrim, Malahide, and Holmpatrick formations.

Local disseminated dolomite (0.1–0.3 mm crystals) postdating blocky calcite cement is present in the Feltrim Formation mud-mound facies, and in Malahide and Lane formation grainstones, where it has planar texture (Sibley and Gregg, 1987) (Fig. 9B) and dark to bright red-orange CL zoning (Fig. 9D). Pervasive replacement dolomite present in the Feltrim, Malahide, Loughshinny, and Holmpatrick formations is medium to coarse-crystalline (0.2 to > 1.0 mm) with nonplanar texture, and is spatially associated with faults as described above. It is inclusion-rich, partially retentive to fully destructive of depositional textures, and typically displays dull-dark red CL (e.g., Figs. 9E–G, 11E, F). Massive dolomitization of the Lane Formation is not seen at surface exposures but is recorded in boreholes (Nolan 1986).

Tournaisian and Viséan strata are cut by millimeter–decimeter wide veins cemented by dolomite and/or calcite. Dolomite-only veins are rare, whereas calcite-only veins are common (Fig. 4A, C, D). Where both are present, pale yellow/brown to white, medium- to coarse-grained (0.5 to 1

TABLE 2.—Summary of data for primary and pseudosecondary fluid-inclusion populations defined by  $T_h$  and  $T_m$  ranges in calcite and quartz veins hosted in Tournaisian and Viséan strata (see Fig. 13).

Locality/Formation	Mineral	$T_h$ °C	$T_m$ °C	Salinity wt. % equiv. NaCl
<b>Howth (Tournaisian)</b>				
Feltrim Fm.	Vein calcite (H-6, 7)	87 to 283 (n = 35)	−25.2 to −1.1 (n = 29)	25.7 to 1.9
Claremont Strand				
Feltrim Fm.	Vein calcite (H-2)	85 to 155 (n = 12)	−26.6 to −0.6 (n = 11)	26.6 to 1.1
Southwest Coast				
<b>Malahide (Tournaisian)</b>				
Malahide Fm.	Vein calcite (M-2C)	86 to 132 (n = 13)	−31.0 to −13.8 (n = 13)	29.3 to 17.6
		85 to 165 (n = 6)	−10.9 to −3.2 (n = 6)	14.7 to 5.3
		205 to 226 (n = 5)	−32.6 to −19.3 (n = 5)	30.4 to 21.9
Tober Colleen Fm.	Vein calcite (M-1B)	243 to 269 (n = 4)	−23.4 to −24.3 (n = 2)	25.1 to 24.6
<b>Loughshinny (Viséan)</b>				
Loughshinny Fm.	Late yellow CL (L-3, 5 & 6)	60 to 156 (n = 50)	−39.8 to −11.8 (n = 38)	35.9 to 15.8
Coppermine Fault	Early zoned-CL (L-5 & 6)	167 to 310 (n = 10)	−13.4 to −5.1 (n = 7)	15.8 to 8.0
		243 to 246 (n = 3)	CO <sub>2</sub> -bearing (n = 3)	8.3 to 7.4
Holmpatrick Fm.	Non-CL quartz (L-10)	151 to 333 (n = 21)	−7.0 to −0.1 (n = 16)	10.5 to 0.2

mm, locally  $\leq 5$  mm) rhombohedral to saddle-shaped dolomite is succeeded by white, coarse-grained (1 to  $> 10$  mm), inclusion-rich blocky calcite spar. Both cements also occur in centimeter–decimeter sized vugs locally present within the fault-associated pervasive dolomitization. They also occur in zebra sheet pores in the Feltrim Formation near the HHF, the Loughshinny Formation near the Coppermine Fault, and locally in the lower Holmpatrick Formation (Figs. 3, 5, 6). In thin section, the dolomite is turbid and displays slight to pronounced undulatory extinction. Infrequently (e.g., in the Malahide Formation and in the Feltrim Formation at Howth) the crystals are crudely banded, with three or four dark zones of Fe-oxide and patchy bright-CL calcite, presumably produced by corrosion and oxidation of relatively ferroan dolomite zones (partial dedolomitization, cf. Hendry et al. 2015) (Fig. 10A, B).

An important characteristic of the dolomite cement is its inconsistent CL zonation, which varies both geographically and stratigraphically. In the Feltrim Limestone at Howth, dolomite cements have a bright red inner core followed by an  $\sim 1.0$ -mm-thick dark zone, a bright red zone of similar thickness, and a thin dark outer zone (Fig. 10C, D). At Malahide, in the eponymous formation, they show alternating moderately bright and dull red zones on an  $\sim 5$  mm scale with fine-scale brighter calcite replacement in the outer zones (Fig. 10A, B). Dolomite cement in the Holmpatrick Formation displays an inner zone of multiple dark and bright red bands followed by a thicker ( $\sim 0.2$  mm) non-luminescent zone (Fig. 10E, F). In vugs and zebra fabrics of the Loughshinny Formation along and close to the Coppermine Fault, as well as in the Drumanagh Member clasts, dolomite cements show thin ( $< 0.1$  mm), alternating bright red CL and non-CL zones (Fig. 10G, H). The CL microstratigraphy is closer to that in the Holmpatrick Formation than to the Tournaisian examples, yet not identical. In general, the cements in Tournaisian strata have fewer, thicker, bright and dark CL zones while those in Viséan strata have more numerous, thinner, alternating bright red and non-CL zones (Fig. S1).

Quartz veins in the Loughshinny Formation associated with the Coppermine Fault consist of black chalcedony overgrown by colorless to pale gray blocky quartz, and lastly very coarse grained (centimeter-scale) white equant quartz (Fig. 11A). Chalcopyrite is locally present in the first two precipitates (Fig. 11B). Dolomite and subsequent calcite cement postdates the quartz. The blocky quartz has thin dark blue and brown CL concentric zones plus sectoral zoning, whereas the equant quartz is dull yellowish brown in CL and the chalcedony is very dark (Fig. 11C, D). Quartz cement filling veins in the Holmpatrick Formation near its basal contact with the Smuggler's Cave Formation is completely black in CL, and its paragenetic context is uncertain owing to a lack of crosscutting

relationships with other quartz, calcite, and dolomite cements. Minor non-CL quartz is also present in veins of the deformed Loughshinny Formation at Loughshinny Harbour, but its relationship to the zoned quartz near the Coppermine Fault is unclear.

The final diagenetic precipitates in the studied strata are calcite vein- and vug-filling cements. Calcite is always later than saddle dolomite where both are present. In Tournaisian strata, the calcite is either fibrous (Malahide Formation) or coarsely crystalline ( $\sim 1$  mm to  $> 1$  cm) and turbid (Feltrim Formation), with numerous solid and fluid inclusions. The calcite is typically a uniform bright orange-brown in CL, with early stages of growth rarely marked by alternating slightly duller and brighter zones (Fig. 11E–H). Likewise, in the Viséan Holmpatrick Formation, coarse blocky calcite overgrowing dolomite cement has a mottled to banded dull to bright orange CL fabric (Fig. 10E, F). Milky white calcite cement in vein and fracture swarms of the folded Loughshinny Formation is also uniform bright orange in CL. In contrast, en-echelon veins in the Lane Formation are filled by turbid calcite with numerous solid inclusions and deformation twins, which are dark brown in CL, except for minor bright yellow alteration along cleavages (Fig. 9G).

The petrographic characteristics and field relationships outlined above define a paragenesis of mineral deposition and faulting and/or fracturing events for the Tournaisian and Viséan strata of the northeast Dublin coast (Fig. 12). While there is much commonality in the early diagenetic calcite cementation and replacive dolomitization, the later diagenesis is more complex in the Viséan and especially associated with the Coppermine Fault. Moreover, although dolomite cements in all the locations and formations have a similar paragenetic context, they have been shown to have significantly distinct CL zonation fabrics. It is noteworthy that none of the CL patterns can be reconciled with the regionally conservative CL microstratigraphy (pk2) described by Wright et al. (2001, 2003) for dolomite cements in Lower Carboniferous carbonate rocks throughout the Irish Midlands and the Dublin Basin (Fig. S1). Otherwise the paragenesis in Figure 12 is similar to that described in the Irish Midlands with a few caveats: (i) void-filling evaporites predating dolomitization are absent; (ii) there is a more restricted distribution of planar replacive dolomite; (iii) post-dolomitization fracture-filling calcite and dolomite cements are more abundant; (iv) sulfide mineralization is limited to the Coppermine Fault and dominated by Cu (with atypically abundant quartz) rather than by Pb-Zn; and (v) final-stage hydrocarbon is absent (Gregg et al. 2001; Nagy et al. 2004; Wilkinson 2010).

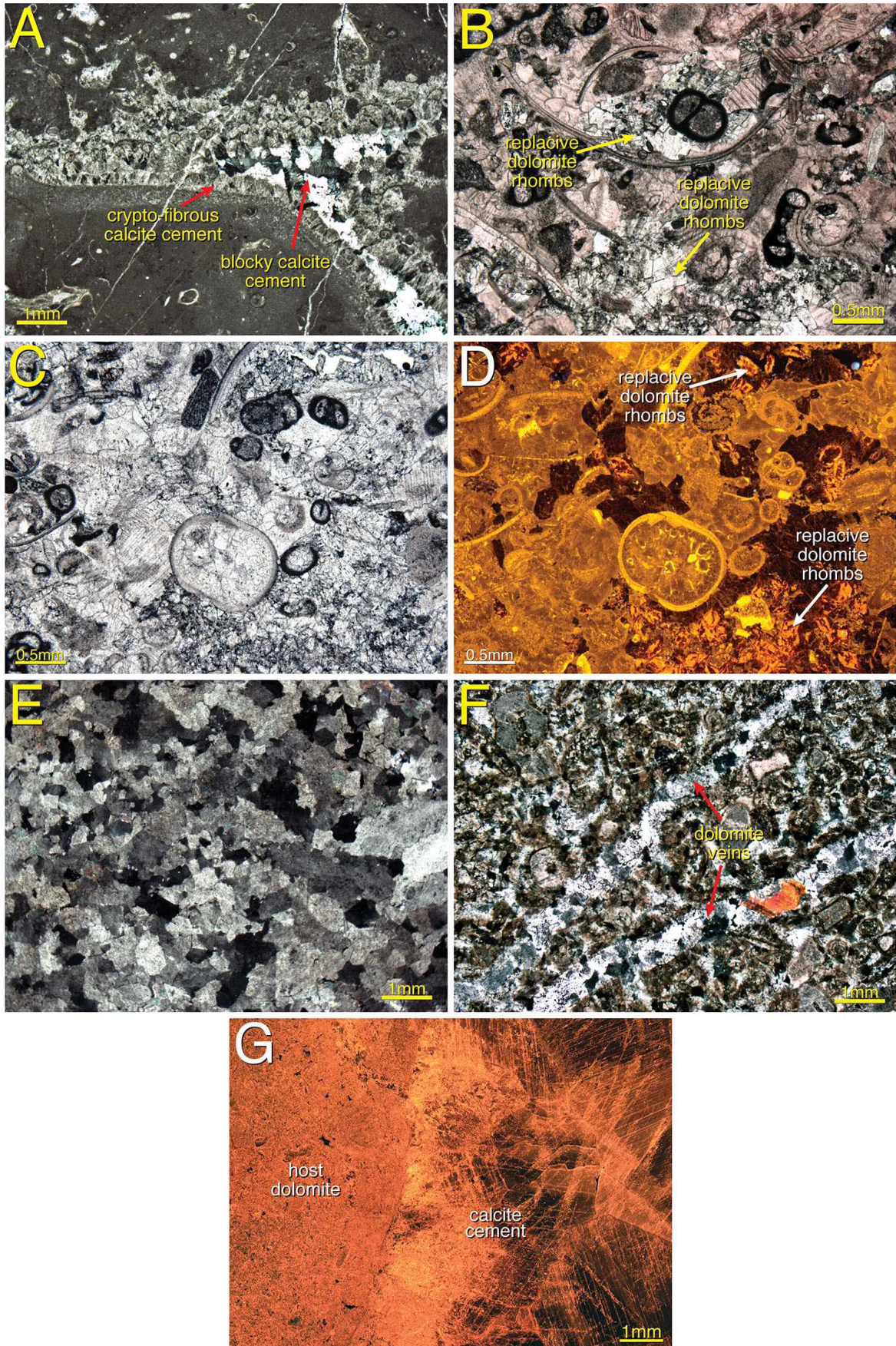
Replacive and pore-filling dolomites and calcite veins described here from the north Dublin coast are spatially closely associated with faults.

TABLE 3.—Carbon, oxygen, and strontium isotope data for carbonate veins and Carboniferous host rocks of the north Dublin coast.

Sample	Formation	Mineral Type	$\delta^{13}\text{C}$ ‰ VPDB	$\delta^{18}\text{O}$ ‰ VPDB	$^{87}\text{Sr}/^{86}\text{Sr}$	Sr (ppm)
<b>Howth (Tournaisian)</b>						
H-1A	Feltrim	weakly dol host ls	-7.20	-5.19	0.709564	7
H-1B	Feltrim	white vuggy cc vein	-6.49	-5.68	0.709207	6
H-1C	Feltrim	dol host ls	-7.61	-4.59		
H-1C	Feltrim	dol host ls dupl	-7.59	-4.64		
H-2A	Feltrim	brown dol host ls	+1.09	-9.66	0.709221	25
H-2B	Feltrim	gray cc vein	-0.88	-13.39		
H-3A	Feltrim	host ls	-7.04	-5.33		
H-3B	Feltrim	brown zebra dolomite	+2.47	-8.66		
H-4A	Feltrim	dol host ls	+3.16	-10.46	0.708940	47
H-4B	Feltrim	vug-filling cc	-7.32	-5.32		
H-5A	Feltrim	weakly dol host ls	+1.90	-5.03		
H-5B	Feltrim	white cc vein	+4.01	-2.88		
H-6A	Feltrim	gray host ls	+3.74	-4.23		
H-6B	Feltrim	vug-filling dolc	-0.17	-6.21	0.708230	75
H-6C	Feltrim	later vug-filling cc	+3.44	-4.26		
H-6D	Feltrim	recrystallized host ls	+3.32	-3.81		
H-7A	Feltrim	30 cm wide cc vein	+2.36	-10.42		
H-8A	Feltrim	host ls	+3.66	-3.36		
H-8B	Feltrim	vug-filling dolc	+2.06	-7.38	0.708382	103
H-8C	Feltrim	white-gray cc vein	+3.09	-5.82		
H-9A	Malahide	host ls	-3.59	-7.59		
H-9A	Malahide	host ls dupl	-3.70	-7.75		
H-9A	Malahide	host ls dupl	-3.48	-7.43		
H-9B	Malahide	white vug-filling cc	+0.42	-16.33	0.710142	499
<b>Malahide (Tournaisian)</b>						
M-1A	Tober Colleen	host ls	+2.77	-8.01	0.710639	582
M-1B	Tober Colleen	white cc vein	+1.93	-8.14	0.708819	1551
M-2A	Malahide	host ls	+1.56	-9.13		
M-2B	Malahide	fibrous white cc vein	+0.64	-12.39		
M-2C	Malahide	white cc vein	+0.79	-11.26		
M-3A	Malahide	brown cc vein	-0.84	-8.71	0.709115	15
M-3B	Malahide	gray cc vein	-0.88	-13.20		
MH-2-5	Malahide*	dol host ls	+0.7	-8.8		
MH-2-6	Malahide*	vug-fill dolc	+1.7	-7.6		
<b>Loughshinny (Viséan)</b>						
L-1A	Loughshinny	host ls	+0.19	-8.48	0.708048	563
L-1B	Loughshinny	early folded cc vein	-1.76	-8.55	0.708034	2359
L-1C	Loughshinny	late white cc vein	-3.50	-11.52	0.709828	80
L-1D	Loughshinny	late white cc vein	-1.22	-14.83		
L-1D	Loughshinny	late white cc vein dupl	-1.24	-14.61		
L-2A	Loughshinny	host ls	-1.56	-9.62		
L-2B	Loughshinny	late white cc vein	-1.22	-14.63	0.708275	527
L-4A	Loughshinny	dol host lst with mal	-0.43	-10.86		
L-6A	Loughshinny	qtz-vein-related dolomite	+0.85	-10.77	0.709542	25
L-7A	Drumanagh Breccia	dol host lst	+0.34	-10.40	0.708520	48
L-7B	Drumanagh Breccia	vein-filling dolc	-0.97	-13.49	0.708992	24
L-8A	Lane	host ls block	+1.19	-8.11		
L-8B	Lane	white cc vein	+2.40	-10.90		
L-8C	Lane	host ls matrix	+1.55	-7.85		
L-9A	Lane	host ls	+2.26	-5.98		
L-9B	Lane	fibrous yellow cc vein	-2.07	-13.57		
L-9C	Lane	host ls	+1.41	-7.64		
L-9D	Lane	fibrous white cc vein	-1.29	-15.00		
L-11A	Holmpatrick	dol host ls	+2.80	-11.20	0.709221	29
L-11B	Holmpatrick	brown dol host ls	+3.03	-11.07	0.708964	25
L-11C	Holmpatrick	cc vein	-3.14	-17.55		
L-12A	Holmpatrick	host ls	+2.95	-6.35		
L-12B	Holmpatrick	fibrous cc vein	+0.74	-13.99		
L-13A	Holmpatrick	host ls	+2.36	-6.62		
L-13B	Holmpatrick	white cc vein	-1.01	-19.79		
L-13C	Holmpatrick	later gray cc vein	-1.07	-21.84		
L-13D	Holmpatrick	recrystallized host ls	-3.12	-12.74		
L-13E	Holmpatrick	brown-yellow cc vein	-1.71	-20.06	0.710639	250

cc, calcite cement; dolc, dolomite cement; dol, dolomitized; ls, limestone; mal, malachite; qtz, quartz; dupl, duplicate.

\* Dolomitized host rock and cement samples from the Malahide Limestone, analyzed by Wright (2001).



Studies elsewhere have shown that such structural conduits may be exploited by chemically distinct fluids over time and space (e.g., Hendry et al. 2015; Mohammadi et al. 2019a, 2019b). This will be examined further, by integrating fluid inclusion and stable-isotope data.

#### FLUID INCLUSIONS

Fluid inclusions suitable for thermometric analysis were present in calcite veins in Tournaisian strata at Malahide and Howth, and in quartz veins in Viséan strata at Loughshinny, but inclusions in dolomite cements were too small for analysis ( $< 2 \mu\text{m}$ ), and calcite veins in Viséan strata were either fibrous and deformed, or contained mostly very small inclusions ( $< 0.5 \mu\text{m}$ ) with sporadic larger inclusions that were dark, deformed and/or ruptured. All inclusions measured were two-phase (vapor + liquid), with shapes ranging from oblate to elongate spheroids and diameters from 2 to 35  $\mu\text{m}$  (most between 3 and 10  $\mu\text{m}$ ). The vast majority have vapor:liquid (V/L) ratios between 0.1 and 0.3, with those whose  $T_h$  values were  $< 200^\circ\text{C}$  typically having ratios generally closer to 0.2 and those with lower  $T_h$  values having ratios closer to 0.1. Microthermometry data are summarized in Table 2.

#### Calcite Veins

Calcite veins in the Malahide Formation close to the North fault (Fig. 3) have inclusions that are  $> 2$  to 10  $\mu\text{m}$  in diameter, with larger ones irregularly shaped. The V/L ratios are highly variable ( $< 0.1$  to  $> 0.4$ ) though most are  $< 0.3$ . Inclusions in the Tober Colleen Formation near the Carrickhill Fault (Fig. 3) generally proved unsuitable for analysis due to scarcity and small size ( $< 2 \mu\text{m}$ ), but limited data were obtained from inclusions in small clear areas of calcite. Combined  $T_h$  values range from 85 to 269°C and  $T_m$  values from  $-3.2$  to  $-32.6^\circ\text{C}$ , reflecting salinities of 5.3 to 30.4 equiv. wt. % NaCl (Fig. 13A). The highest  $T_h$  values (243 and 269°C) come from the samples close to the Carrickhill Fault. There is no correlation between V/L ratios and  $T_h$  values.  $T_e$  values of  $-50$  to  $-23^\circ\text{C}$  indicate the presence of both NaCl–CaCl<sub>2</sub>–H<sub>2</sub>O and NaCl–H<sub>2</sub>O–type brines (Crawford 1981; Zhang and Frantz 1989).

Inclusions in vug-filling calcite cements and white to gray calcite veins cutting the Feltrim Formation limestones at Howth near Sutton Dinghy Club and along Claremont Strand (Fig. 5) have  $T_h$  values from 85 to 283°C and  $T_m$  values from  $-0.6$  to  $-26.6^\circ\text{C}$ , reflecting salinities of 1.1 to 26.6 equiv. wt. % NaCl (Fig. 13A). Eutectic melting temperatures ( $T_e$ ) of  $-21$  to  $-52^\circ\text{C}$  indicate the presence of NaCl–H<sub>2</sub>O brines as well as more complex brines that likely also contain CaCl<sub>2</sub>. Inclusions with intermediate  $T_h$  values (between 150 and 185°C) have  $T_e$  values that indicate only NaCl–H<sub>2</sub>O–type brine, whereas those with higher and lower  $T_h$  values tend to have  $T_e$  values that record the presence of both types of brines.

There is a clear relationship between  $T_h$  values and salinity for the fluids from the calcite veins (Fig. 13A). Most plot along a crude covariant trend between two end members: a lower-temperature, higher-salinity fluid ( $T_h$  values of 88 to 130°C,  $T_m$  values between  $-30$  and  $-20^\circ\text{C}$  corresponding to salinities  $> 22$  wt. % equiv. NaCl) and a higher-temperature, lower-salinity fluid ( $T_h$  values of 175 to 260°C,  $T_m$  values of  $-6$  to  $0^\circ\text{C}$ , corresponding to salinities  $< 9$  wt. % equiv. NaCl). The low-salinity data show greater scatter, extending to lower temperatures ( $T_h$  values of 85 to 115°C) that

might reflect the presence of a third fluid or represent a cooling and/or mixing trend. Data from inclusions at Malahide generally show more scatter than those from Howth, although there is a similar lower-temperature, higher-salinity cluster ( $T_h = 86$  to  $132^\circ\text{C}$ ,  $T_m < -20^\circ\text{C}$ , corresponding to  $> 22$  wt. % equiv. NaCl) that trails off towards lower salinities and only slightly higher temperatures ( $T_h = 86$  to  $132^\circ\text{C}$ ,  $T_m = -15$  to  $-3^\circ\text{C}$ , corresponding to  $\sim 19$  to 5 wt. % equiv. NaCl). A distinct high-temperature, high-salinity data cluster unique to Malahide Limestone and Tober Colleen Formation veins at Howth,  $T_h = 205$  to  $269^\circ\text{C}$ ,  $T_m = -33$  to  $-19^\circ\text{C}$ , corresponding to  $> 21$  wt. % equiv. NaCl) is not represented elsewhere.

Only five useable inclusions were encountered in calcite veins in the folded Loughshinny Formation at Loughshinny Harbour (Fig. 5). Two secondary inclusions yielded  $T_h$  values of 195 and 200°C and  $T_m$  values of  $-14.3$  and  $-14.5^\circ\text{C}$ , corresponding to 18.0 and 18.2 equiv. wt. % NaCl, and  $T_e$  values near  $-21^\circ\text{C}$  suggesting a NaCl–H<sub>2</sub>O brine. Three other inclusions decrepitated at temperatures of 234 to 280°C.

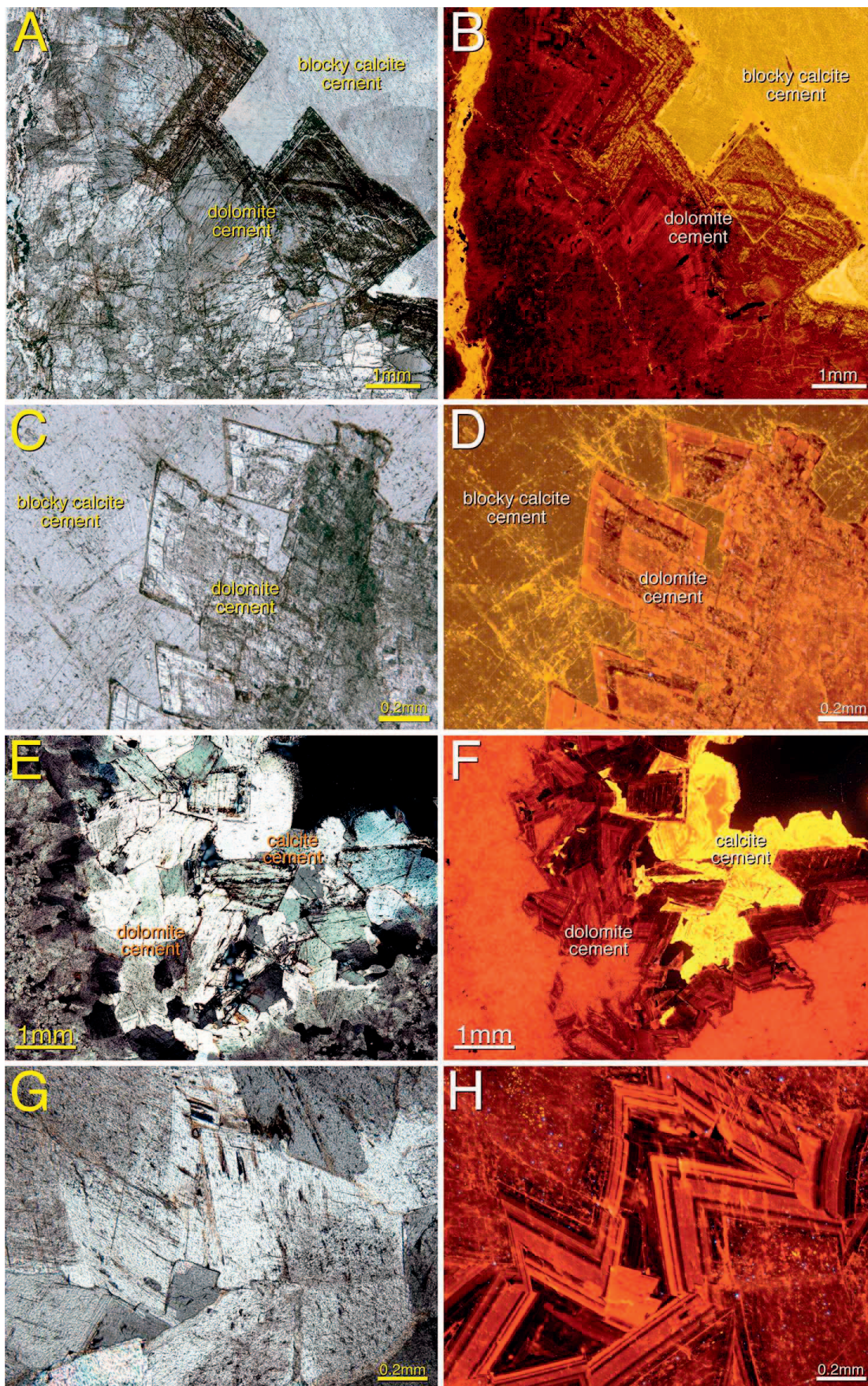
#### Quartz Veins

Inclusions were analyzed from two types of quartz veins at Loughshinny (Fig. 6): decimeter-scale, CL-zoned veins in the Loughshinny Formation along the Coppermine Fault (Fig. 7E), and centimeter- to decimeter-scale white, non-CL veins in the Holmpatrick Formation. Three samples of Loughshinny Formation quartz had primary inclusions 3–10  $\mu\text{m}$  in diameter (rarely up to 35  $\mu\text{m}$ ), plus more elongate pseudosecondary inclusions. All are two-phase aqueous inclusions with V/L ratios near 0.1. CO<sub>2</sub> clathrate melting was observed in three examples, indicating that small amounts of CO<sub>2</sub> were present.  $T_e$  values from  $-33$  to  $-52^\circ\text{C}$  reflect predominantly NaCl–CaCl<sub>2</sub>–H<sub>2</sub>O brine compositions.  $T_h$  values varied from 60 to 310°C and salinities from 7.4 to 35.9 equiv. wt. % NaCl.

Inclusion-laden crystals in microveins from the Holmpatrick Formation reflect multiple fracturing and healing events during quartz emplacement, making it difficult to differentiate primary and pseudosecondary inclusions (Shelton and Orville 1980). Two-phase aqueous inclusions range from 1 to 10  $\mu\text{m}$  with V/L ratios from  $\sim 0.1$  to 0.4 (mode 0.25).  $T_e$  values are approximately  $-22^\circ\text{C}$ , indicating a NaCl–H<sub>2</sub>O brine.  $T_h$  values range from 151 to 333°C and  $T_m$  values from 0.0 to  $-7.0^\circ\text{C}$ , reflecting low to moderate salinities of 0.0 to 10.5 equiv. wt. % NaCl.

The quartz data define a covariation between lower-temperature, higher-salinity fluids ( $T_h = 60$  to  $128^\circ\text{C}$ ,  $T_m = -21.8$  to  $-38.2^\circ\text{C}$ , corresponding to  $> 22$  wt. % equiv. NaCl) in the Loughshinny Formation, and higher-temperature, lower-salinity fluids in the Holmpatrick Formation ( $r = -0.82$  [significance  $> 0.99$ ], Fig. 13B). However, there is a cluster at moderate temperatures and salinities ( $T_h = 85$  to  $176^\circ\text{C}$ ,  $T_m$  between  $-16.3$  and  $-11.7^\circ\text{C}$ , corresponding to  $\sim 20$  to 16 wt. % equiv. NaCl), whereas several inclusions define a distinct high temperature ( $T_h > 250^\circ\text{C}$ ) fluid of moderate salinity ( $T_m = -13.4$  to  $-11.7^\circ\text{C}$ , corresponding to  $\sim 16$  wt. % equiv. NaCl). There is no relationship of  $T_h$  values to quartz petrographic zonation. The three CO<sub>2</sub>-bearing pseudosecondary inclusions record high temperature and low salinity ( $T_h = 243$  to  $246^\circ\text{C}$ , 7.4 to 8.3 equiv. wt. % NaCl, based on clathrate melting) (e.g., Diamond 1992).

Fig. 9.—Petrographic fabrics in Mississippian limestones on the north Dublin coast. **A**) Stromatactis cavity in the Feltrim Limestone Formation filled by a cryptofibrous early generation of calcite cement nucleating in part on fenestellid bryozoan fronds, followed by blocky calcite cement (Claremont Strand, Howth, cross-polarized light [XPL]). **B**) Partially dolomitized grainstone of the Lane Formation. Calcite is stained with alizarin red S; planar-dolomite patches remain unstained. **C, D**) PPL and CL images of Lane Limestone showing fossil debris (foraminifera, crinoid and ostracod, bottom center). Early bright, dull and dark CL blocky calcite cements were precipitated likely under variable redox conditions. A cluster of replacive dolomite rhombs is labeled, which is red-orange compared to yellow-orange of calcite cement. Other replacive dolomite rhombs are visible scattered throughout the sample. **E**) Grainstone of the Malahide Formation replaced by nonplanar dolomite. Original crinoid skeletal grains are preserved as ghosts in nonplanar-dolomite matrix, which is cut by dolomite-cement-filled veins (XPL). **F**) Nonplanar replacement dolomite fabric in the Drumanagh Member (XPL). **G**) CL image of non-CL calcite vein cement overgrowing dull red CL host nonplanar dolomite of the Lane Formation. The calcite displays bright-CL alteration along cleavages.



## STABLE ISOTOPES

Carbon and oxygen isotope data for carbonate samples encompass a very wide range of  $\delta^{18}\text{O}$  (–2.9 to –22.9‰) and  $\delta^{13}\text{C}$  (+4.0 to –7.6‰) values (Table 3). On a cross plot (Fig. 14A) the overall pattern is a crude positive covariance with a secondary trend towards lower  $\delta^{13}\text{C}$  but relatively high  $\delta^{18}\text{O}$  values. Strontium isotope data range from 0.708034 to 0.710639 (Table 3) and are plotted against  $\delta^{18}\text{O}$  values from the same samples in Figure 14B. The data are poorly correlated, although the highest  $^{87}\text{Sr}/^{86}\text{Sr}$  value is from the most  $^{18}\text{O}$ -depleted sample. Most of the values are significantly more radiogenic than those from carbonates precipitated in equilibrium with Mississippian seawater (Mii et al. 1999).

Considering the data in Figure 14A in terms of sample type, age of host strata, and general location (Tournaisian at Howth and Malahide, Viséan at Loughshinny; Figs. 3, 4, 6) draws out several patterns. Most of the host limestones define a cluster in C-O isotope space with  $\delta^{18}\text{O}$  values between –3.4 and –9.1‰ and  $\delta^{13}\text{C}$  between +3.7 and +1.2‰. The most  $^{18}\text{O}$ -enriched samples overlap the range of Mississippian marine calcites that formed in equilibrium with ambient seawater (Mii et al. 1999), and all of these are from the Feltrim Formation at Claremont Strand, Howth. Oxygen and carbon isotope values are lower for Loughshinny, Lane, and Holmpatrick Formation samples, with the lowest  $\delta^{18}\text{O}$  value from the Malahide Formation. These are bulk samples, inevitably containing some diagenetic cement with a lower  $\delta^{18}\text{O}$  content than the depositional carbonate components, so some values lower than pure primary marine calcites are to be expected despite careful sampling. Relatively more diagenetic contamination is likely in grainy Malahide and argillaceous–bioclastic Tober Colleen Formations than in the originally lower-porosity mud-mound micritic limestones of the Feltrim Formation, which may account for their generally slightly more negative  $\delta^{18}\text{O}$  values.

Several samples from Howth fall outside the main data cluster, having similar oxygen but much lower carbon isotope values. These are all samples from locations close to the HHF; the Feltrim Formation at Sutton in the SW of the Howth peninsula, and the Malahide Formation at Balscadden Bay on the NE (Fig. 5). The latter are relatively lower in  $\delta^{18}\text{O}$  value (~ –7.6‰ versus ~ –5.3‰) but have less negative  $\delta^{13}\text{C}$  values (~ –3.5‰ versus ~ –7.1‰). Two limestones from the Loughshinny Formation also plot as outliers to the main data cluster, with  $\delta^{18}\text{O}$  values of –9.6 and –12.7‰, and  $\delta^{13}\text{C}$  values of –1.6 and –3.1‰. Petrographically, both samples display evidence of intense recrystallization (e.g., Folk 1965).

Dolomitized limestones and dolomite cement compositions mutually overlap, with  $\delta^{18}\text{O}$  values between –6.2 and –11.2‰ and  $\delta^{13}\text{C}$  values between +3.6 and –0.8‰. One exception, a partially dolomitized limestone from the Feltrim Formation at Sutton (Howth) has less negative  $\delta^{18}\text{O}$  (–4.6‰) and more negative  $\delta^{13}\text{C}$  (–7.6‰) values, similar to that of limestones at the same location. Another pervasively dolomitized limestone from Sutton falls in the main dolomite data field ( $\delta^{18}\text{O}$  and  $\delta^{13}\text{C}$  values of –10.5‰ and +3.2‰ respectively). An additional outlier in C-O isotope space is a dolomite vein cement from the Drumanagh Member near the Coppermine Fault that has an atypically low  $\delta^{18}\text{O}$  value of –13.5‰ and a slightly lower  $\delta^{13}\text{C}$  value of –1.0‰ (some sample contamination by later calcite cement can't be ruled out).

Although the dolomite isotopic data intersect the range for host limestones, their different isotopic fractionation factors need to be

considered in any interpretation. Dolomite precipitated from the same seawater as calcite at 25°C should plot approximately 3 to 4‰ heavier with respect to  $\delta^{18}\text{O}$  (Land 1980; Woronick and Land 1985), with the difference decreasing to around 2‰ at ~ 100 to 200°C (Horita 2014). In Figure 14C the dolomite values are conservatively shifted by –2‰ to represent calcites that would have precipitated in equilibrium with the same parent fluids. The adjusted values fall outside the field for host limestones, indicating that the dolomites did not form syndepositionally. Petrographically, all the analyzed dolomites display nonplanar texture, although samples from the Feltrim Formation at Howth also contain some (presumably) earlier diagenetic planar dolomite.

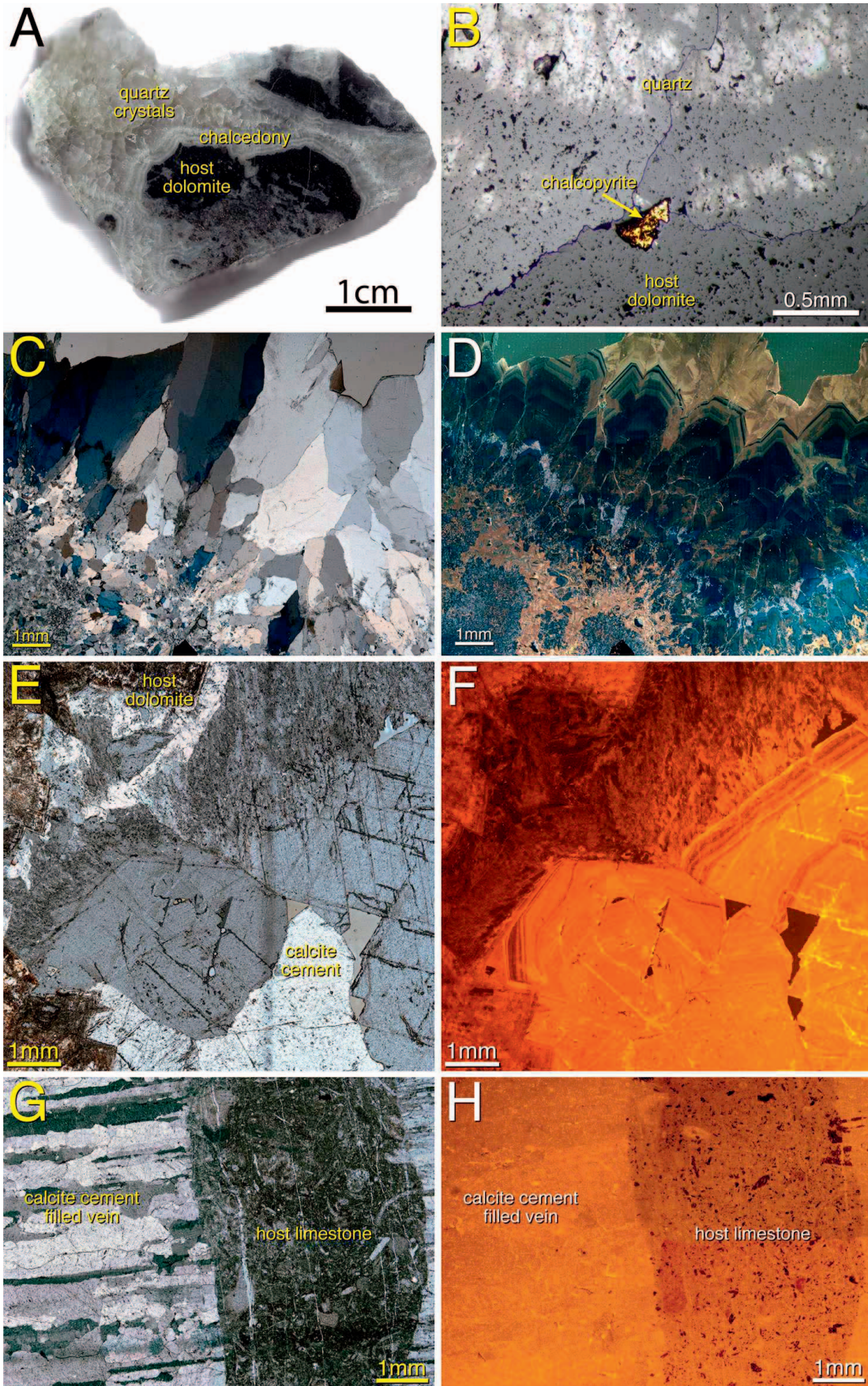
Three quartz-vein samples were analyzed for oxygen isotope composition. CL-zoned limpid quartz and later white overgrowths associated with chalcopyrite along the Coppermine Fault, Loughshinny, yielded  $\delta^{18}\text{O}$  values of +16.0 and +15.1‰ VSMOW, respectively. White, non-CL quartz associated with faults in the lower Holmpatrick Formation gave a value of +16.3‰.

Calcite cements from veins and vugs show a very wide range in  $\delta^{18}\text{O}$  (–2.9 to –21.9‰) and  $\delta^{13}\text{C}$  (+4.0 to –7.3‰) values (Fig. 14A). The  $^{18}\text{O}$ -enriched end of the data field consists of vug and vein-fill cements in Tournaisian strata at Howth that have O and C isotope compositions very similar to their local host limestones (including the  $^{13}\text{C}$ -depleted subgroup from close to the HHF). In contrast, the most  $^{18}\text{O}$ -depleted calcite cements are all from the Viséan Holmpatrick Formation at Loughshinny. Calcite cements in Viséan host rocks also tend to have lower  $\delta^{13}\text{C}$  values than those in Tournaisian strata (except for the aforementioned subset from Howth).

Collectively, the stable-isotope results define a paragenetic trend of decreasing  $\delta^{18}\text{O}$  and (to a lesser extent, excepting the subset from Howth) decreasing  $\delta^{13}\text{C}$  (Fig. 14A). Compared to host limestones, dolomites have up to ~ 5‰ lower  $\delta^{18}\text{O}$  values and similar to slightly lower  $\delta^{13}\text{C}$  compositions, while late calcite cements have comparable much lower  $\delta^{18}\text{O}$  and  $\delta^{13}\text{C}$  values, up to ~ 13‰ and ~ 6‰, respectively. Strontium isotope data show considerable overlap between sample types, with lowest values (within the range of Mississippian primary marine calcites) from host limestones, highest values from calcite vein and vug cements, and dolomites or dolomitized limestones giving intermediate values (Fig. 14B). No stratigraphic trends can be drawn from the  $^{87}\text{Sr}/^{86}\text{Sr}$  data set. However, in Tournaisian strata at Howth the highest values are from partly dolomitized limestones at Sutton and calcite veins at Balscadden Bay, both close to the HHF, and the lowest values are from dolomite cements at Claremont Strand far from the HHF.

With respect to the overall paragenesis, Figure 14C documents a general trend of increasing  $^{87}\text{Sr}/^{86}\text{Sr}$  values and decreasing  $\delta^{18}\text{O}$  values with time, also evident from the individual sample locations. However, samples with  $^{87}\text{Sr}/^{86}\text{Sr}$  values in the range of marine calcite in equilibrium with Mississippian seawater still have  $\delta^{18}\text{O}$  values lower than expected for equilibrium marine precipitates. This is exemplified by host limestones and deformed veins from the Loughshinny Formation at Loughshinny Harbour (Fig. 7C, D; Table 3) that have  $^{87}\text{Sr}/^{86}\text{Sr}$  values of 0.70803 to 0.70805 and  $\delta^{18}\text{O}$  values of –9.6 to –8.5‰ (Fig. 13B). Late-stage crosscutting veins have much higher  $^{87}\text{Sr}/^{86}\text{Sr}$  (0.70828 to 0.70983) and lower  $\delta^{18}\text{O}$  (–8.6 to –14.8‰) values. The highest  $^{87}\text{Sr}/^{86}\text{Sr}$  value (0.71064) also has the lowest  $\delta^{18}\text{O}$  (–20.1‰) and is a fault-associated vein calcite from the Holmpatrick Formation at Loughshinny.

Fig. 10.—Petrographic fabrics in Mississippian limestones on the north Dublin coast. **A, B** XPL and CL images of blocky calcite cement overgrowing open-space-filling dolomite in the Malahide Limestone (Malahide, fault Block E of Fig. 3); CL shows zoned dolomite cements (red and dark red) that experienced dedolomitization (bright yellow inclusions). **C, D** XPL and CL images of dolomite cement and later calcite filling open space (Feltrim Limestone Formation, Howth, Claremont Strand); CL shows thick banding in dolomite cements. **E, F** XPL and CL images of open-space-filling dolomite and calcite cements in the lower Holmpatrick Formation. Note the bright compositional zoning in the calcite cement in contrast to the calcite shown in Figure 9G. **G, H** XPL and CL images of dolomite cement in the Drumanagh Member of the Loughshinny Formation.



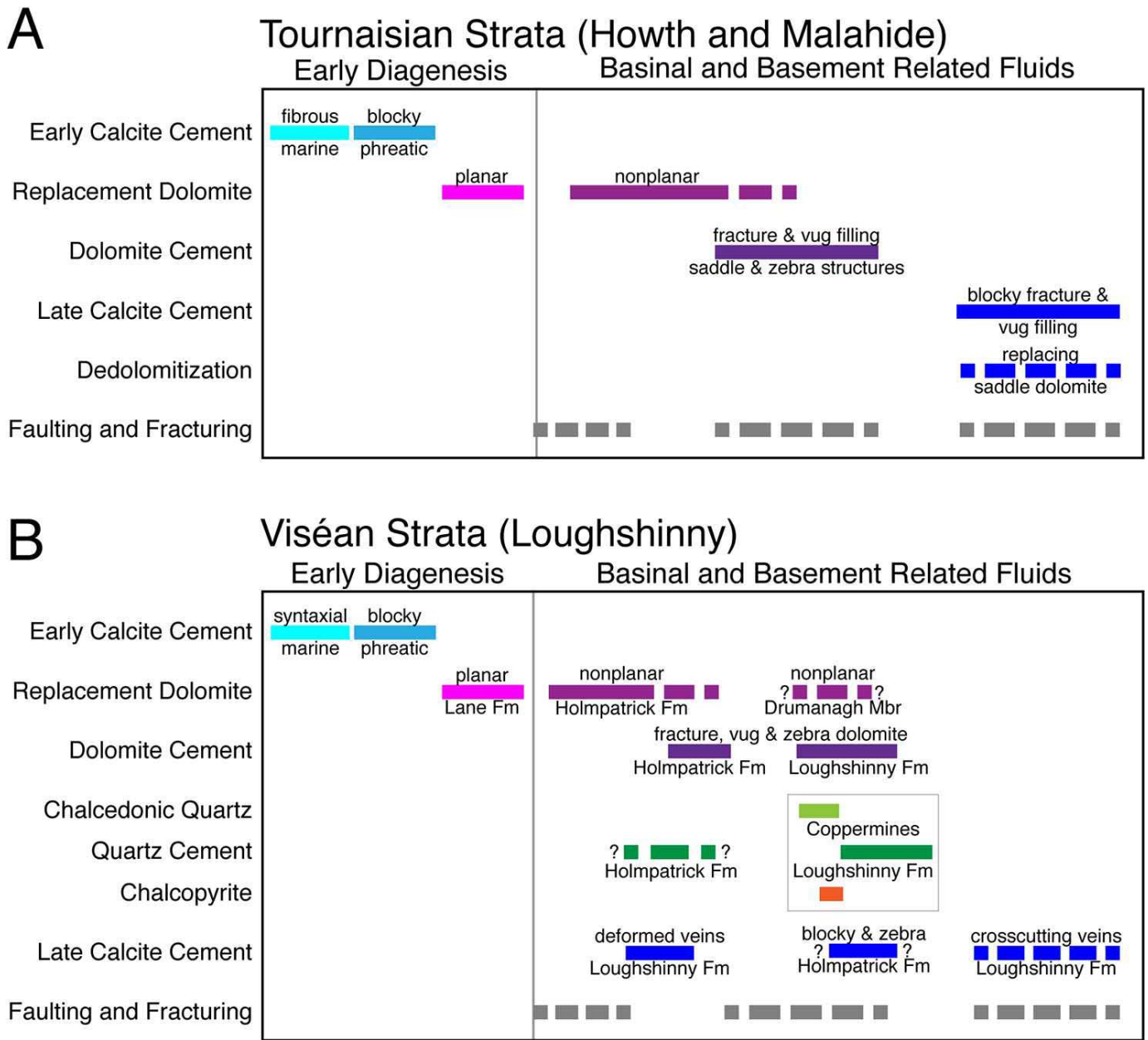


FIG. 12.—Comparative parageneses for early and later fault-related diagenesis of **A)** Tournaisian (Dublin Basin) and **B)** Viséan (Balbriggan Block) strata on the north Dublin coast (Fig. 2).

CHARACTERIZATION AND INTERACTION OF DIAGENETIC FLUIDS

**Fluid-Inclusion Constraints.**—There is considerable scatter in the pooled fluid-inclusion data, but a substantial degree of overlap, suggesting interaction between the common end members (although we cannot rule out similar, but separate, fluids precipitating cements at different times

during multiple fracturing and healing events and/or with pulsed fluid flow). Samples from Tournaisian and Viséan strata record similar lower-temperature, higher-salinity fluid ( $T_h \sim 60$  to  $130^\circ\text{C}$ , typically  $> 22$  wt. % equiv. NaCl, labeled “Pervasive Brine” in Fig. 13C). Analogous hypersaline brines in Carboniferous host strata were present throughout

FIG. 11.—Petrographic fabrics in Mississippian limestones on the north Dublin coast. **A)** Polished slice of vein quartz from the damage zone of the Coppermine Fault, Loughshinny (sample L-3), showing clast-rimming chalcedony followed by equant limpid quartz. Sample is 5 cm across. **B)** Chalcopryrite along contact between quartz vein (top) and dolomitized host rock (bottom) at the Coppermine Fault (reflected PPL). **C, D)** Partial XPL and CL images of zoned quartz vein along the Coppermine Fault. Note the transition from chalcedonic toward coarse euhedral quartz (from bottom toward top) coincident with change in CL character. **E, F)** Partial XPL and CL images of calcite cement overgrowing dolomitized limestone of the Feltrim Limestone Formation (Howth, near Sutton Dinghy Club); CL shows zoning in calcite cements and partial dedolomitization of host rock (blotchy bright yellow bands in the outer zones of the dolomite crystals). **G, H)** XPL and CL images of fibrous calcite vein crosscutting Malahide Formation limestone.

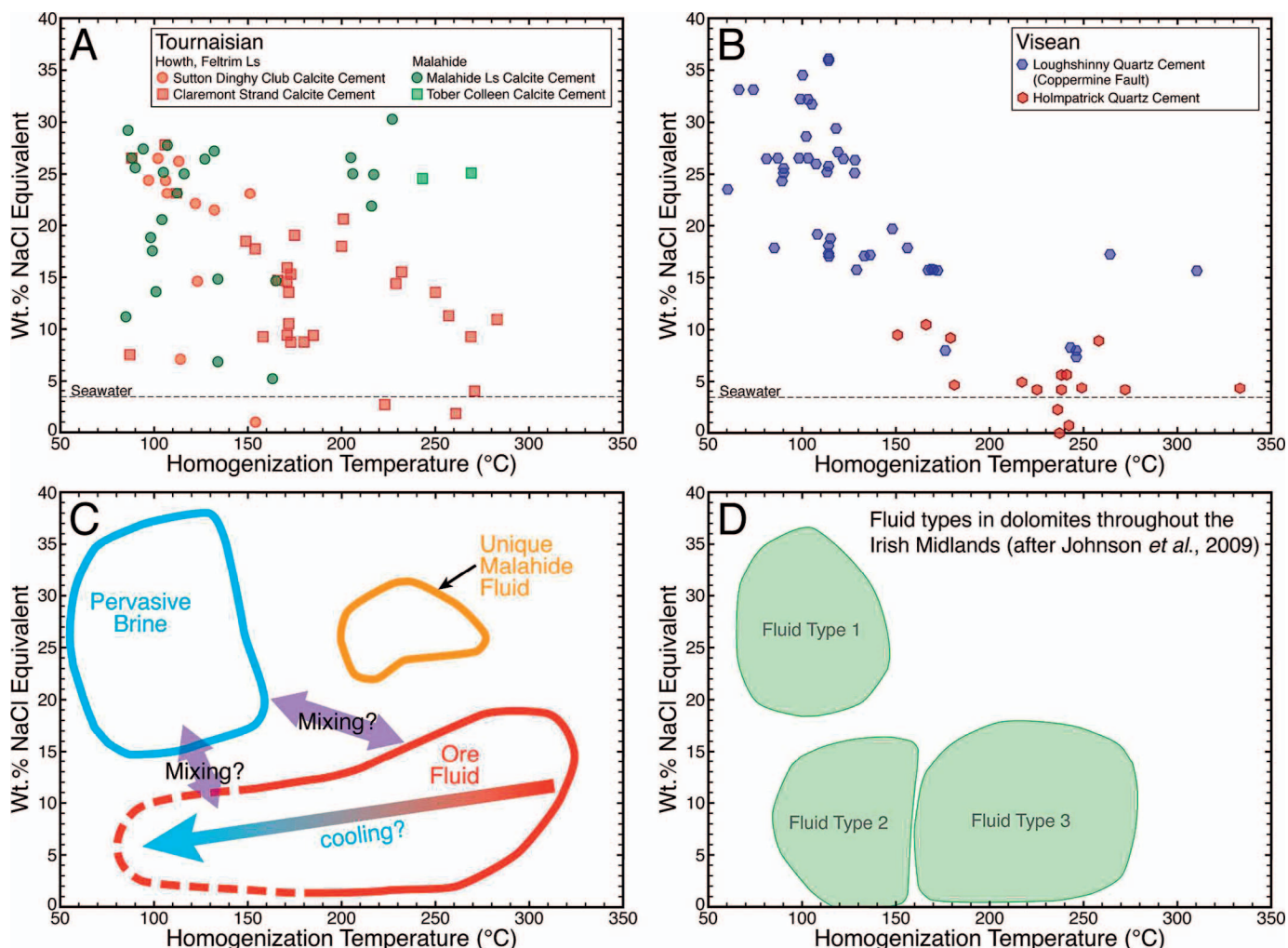


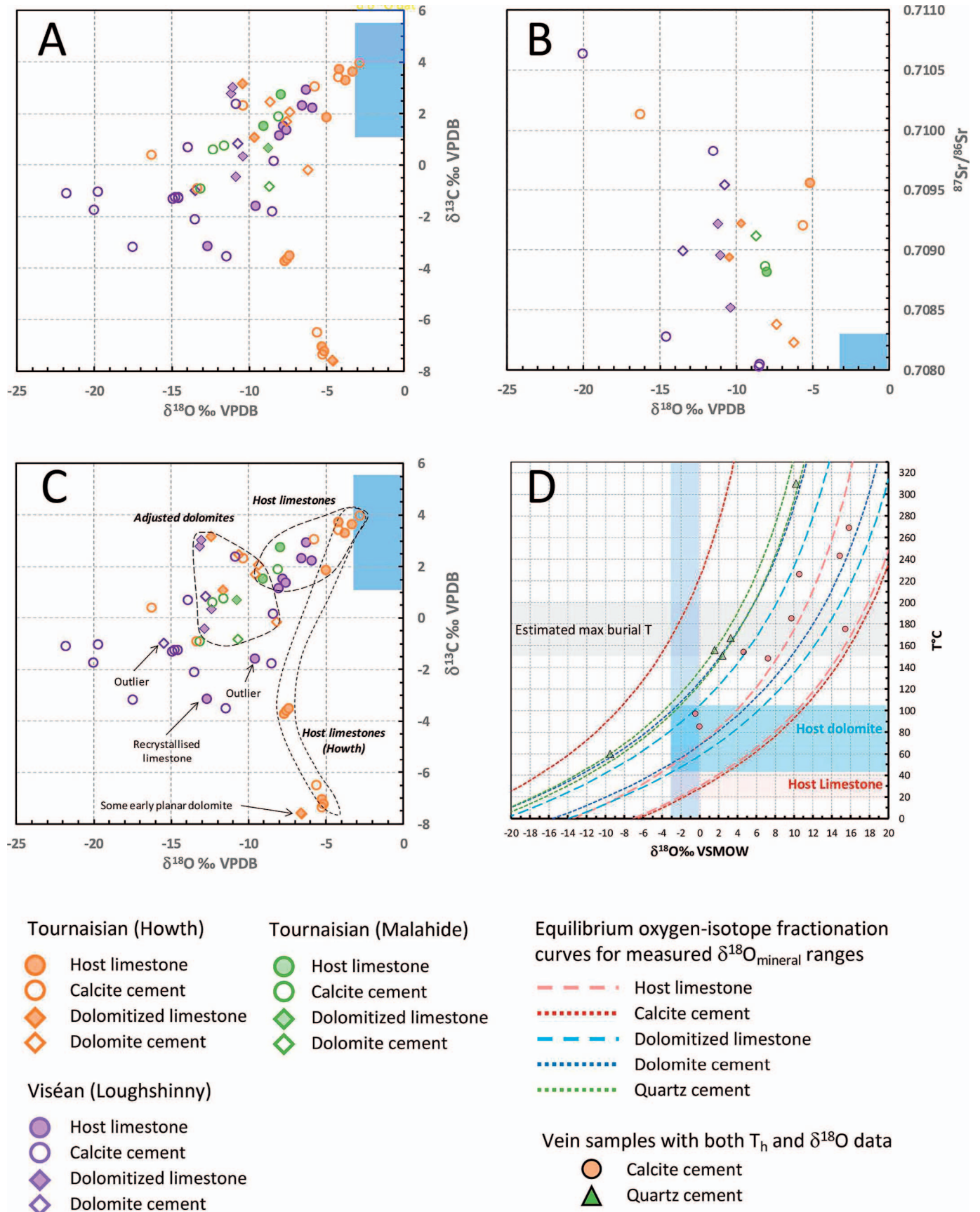
Fig. 13.—Fluid-inclusion homogenization temperature–salinity variation in calcite and quartz veins of the north Dublin coast. **A)** Tournaisian-hosted calcite veins. **B)** Viséan-hosted quartz veins. **C)** Fields showing major fluids in the three localities and inferred cooling and mixing trajectories. **D)** Shaded fields show the three fluid types recognized in dolomites of the Irish Midlands (Johnson *et al.* 2009). Estimated Mississippian seawater salinity in Parts A and B are from Mohammadi *et al.* 2019a, 2019b).

the Irish Midlands (shaded field labeled Fluid Type 1 in Fig. 13D) and may reflect a regional-scale, basal fluid flow system (Johnson 1999; Wright *et al.* 2000; Gregg *et al.* 2001; Johnson *et al.* 2009). However, as noted, dolomites in this study with this fluid signature have a CL microstratigraphy different from that described more regionally.

Data from Howth and Loughshinny define a trend towards a generally higher-temperature and lower-salinity end member ( $T_h \sim 120$  to  $335^\circ\text{C}$ ,  $< 5$  to  $\sim 17$  wt. % equiv. NaCl), with highest temperatures from non-CL vein quartz in the Holmpatrick Formation. These resemble the hot fluids recorded in fault-related non-CL quartz veins on the Isle of Man ( $\sim 125$

km to the NE; Shelton *et al.* 2011), those from ore fluids associated with Zn-Pb sulfide mineralization in Carboniferous-hosted Irish ore systems (Banks *et al.* 2002; Wilkinson and Earls 2000; Wilkinson 2003, 2010), and those in dolomite cements in Carboniferous strata throughout the Irish Midlands (Fluid Type 3 of Johnson *et al.* 2009, Fig. 13D). Moderate-temperature, low- to moderate-salinity fluids captured in zoned quartz of Loughshinny Formation veins at the Coppermine Fault are also strikingly similar to those from complex-CL quartz veins, sphalerite, and saddle dolomite in zinc-sulfide-mineralized Carboniferous breccia on the Isle of

Fig. 14.—Stable-isotope cross plots showing systematic variations among host carbonate, and calcite and dolomite cement, in the north Dublin localities. **A)** Carbon versus oxygen isotope compositions. Blue box shows the range of limestones in equilibrium with Mississippian seawater (Mii *et al.* 1999). **B)** Strontium versus oxygen isotope compositions.  $^{87}\text{Sr}/^{86}\text{Sr}$  and  $\delta^{18}\text{O}$  values co-vary. Vein-filling calcite cements with the lowest  $\delta^{18}\text{O}$  values (approaching  $-20\text{‰}$ ) have the highest  $^{87}\text{Sr}/^{86}\text{Sr}$  values ( $> 0.7105$ ), whereas host limestone and replacement or porefilling dolomite display higher  $\delta^{18}\text{O}$  values ( $\sim -5\text{‰}$ ) and lower  $^{87}\text{Sr}/^{86}\text{Sr}$  values (approaching 0.7080), indicative of host rock buffering of isotope values. **C)** Similar to part A but with  $-2\text{‰}$  adjustment to dolomite  $\delta^{18}\text{O}$  values such that they represent calcites that would have been in equilibrium with the same fluids, emphasizing the general progression toward lower  $\delta^{13}\text{C}$  and  $\delta^{18}\text{O}$  with paragenesis (with the exception of some samples from Howth, discussed in the text). **D)** Equilibrium oxygen isotope fractionation curves for maximum and minimum  $\delta^{18}\text{O}$  values measured from host limestones, dolomitized host limestones, and calcite, dolomite, and quartz vein and vug cements. The blue vertical bar indicates the range of Mississippian seawater  $\delta^{18}\text{O}$  values (Mii *et al.* 1999), the gray horizontal bar shows the approximate range of burial temperatures in the northeast Dublin Basin, and the red and blue horizontal bars show the possible temperature ranges for host limestone and host dolomite if they had formed or recrystallized in ambient seawater. See text for discussion.



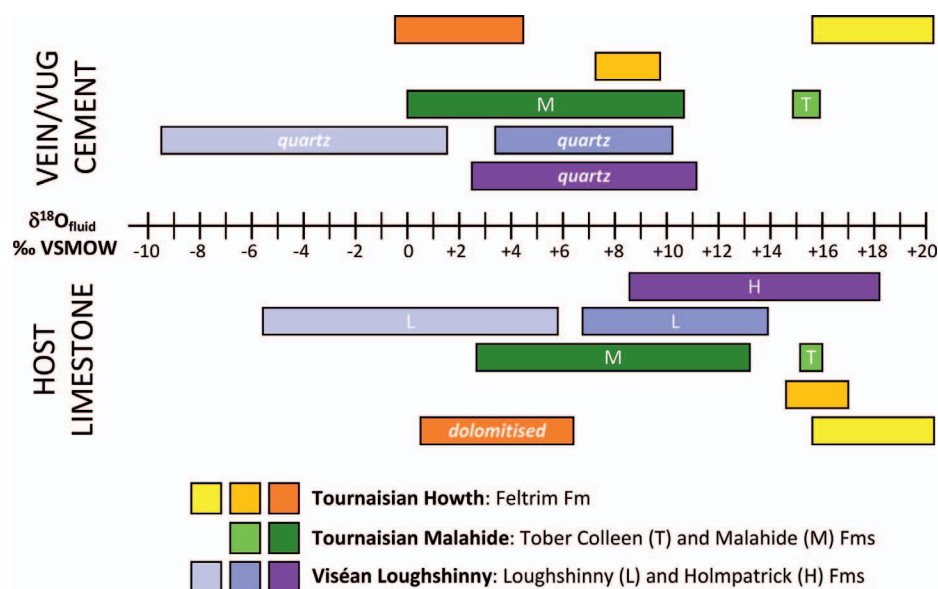


FIG. 15.—Top: Calculated equilibrium ranges of  $\delta^{18}\text{O}_{\text{water}}$  for vein cements (qz = quartz, all other veins are calcite) for which both stable-isotope and fluid-inclusion data are available. Each color represents an individual sample (see Table S1). Bottom: Calculated ranges of  $\delta^{18}\text{O}_{\text{water}}$  that would be in equilibrium with analyzed host limestones adjacent to the same vein cements for the same temperature ranges (see Table S1).

Man (Shelton et al. 2011). These warm to hot fluids are labeled “Ore Fluid” in Figure 13C.

Vein calcites in Tournaisian strata near the Carrickhill Fault at Malahide (Fig. 3) record a distinct high-temperature ( $T_h > 200^\circ\text{C}$ ), high-salinity fluid that has not been recognized elsewhere on the northeast Dublin coast (labeled “Unique Malahide Fluid” in Fig. 13C). More generally, highest  $T_h$  values determined for calcite at both Malahide and Howth are from veins proximal to faults, so it can be hypothesized that the high-temperature–high-salinity fluid represents a portion of the Pervasive Brine that was entrained and heated within a higher-temperature fault-related system.

Intermediate temperature–salinity fluids with compositions between the Pervasive Brine and Ore Fluid end members in Figure 13 could reflect fluid mixing, especially for the pooled Viséan quartz inclusion data that define a negative covariant trend (Fig. 13B). In more detail the quartz cement from the Coppermine Fault shows polymodal  $T_h$  and salinity distributions, and the quartz cement from the Holmpatrick Formation shows partly overlapping bimodal distributions (Fig. S2, see Supplemental Material), suggesting that mixing occurred in discrete pulses. In addition, the fluids trapped in early CL-zoned quartz from the Coppermine Fault are closer in temperature and salinity to those of the Holmpatrick Formation. Tournaisian fluid-inclusion data are too scattered to support a simple two-component mixing trend, suggesting that cooling or additional fluids may be involved (Fig. 13A, C). Correspondingly,  $T_h$  and salinity distributions from calcite-hosted inclusions at both Howth and Malahide show substantially overlapping polymodal distributions (Fig. S2). Variable  $T_h$  values (85 to  $260^\circ\text{C}$ ) for moderate- to low-salinity fluids (< 14 wt. % equiv. NaCl) likely represent cooling of a high-temperature–low-salinity fluid end member, while variation in salinity (from 28 to 6 wt. % equiv. NaCl) for lower temperature fluids ( $T_h = 60$  to  $130^\circ\text{C}$ ) suggests mixing of higher- and lower-salinity end members. Intermediate values would then reflect mixing as fluids cooled over time. An alternative explanation for the lower-temperature, lower-salinity data could be a separate fluid, comparable to the “Type 2” fluid of Johnson et al. (2009) observed in the Irish Midlands, but the lack of a corresponding data cluster argues against this.

**Stable-Isotope Constraints.**—Analyses of host limestone and dolomite, and dolomite and calcite vein and vug cements from Tournaisian and Viséan strata, define a broad paragenetic trend from  $\delta^{18}\text{O}$  values of  $-3$  to  $-22\text{‰}$  and from  $\delta^{13}\text{C}$  values of  $+4$  to  $-4\text{‰}$  (with an atypical low- $\delta^{13}\text{C}$

population at Howth) (Fig. 14A). While  $\delta^{18}\text{O}$  values for host limestone, host dolomite, and dolomite cements overlap considerably, calcite vein cements extend to much lower values. Such a large  $\delta^{18}\text{O}_{\text{mineral}}$  range is unlikely due to temperature alone, especially as fluid-inclusion data have been interpreted to show interaction among compositionally distinct fluids as well as cooling. It follows that calculated  $\delta^{18}\text{O}_{\text{water}}$  values should also be consistent with both geochemical and thermal differences in fluids, either in their sources or in their history of interaction with rocks and/or with other fluids along their flow paths (cf. Shelton et al. 2009, 2011).

Figure 14D shows the possible temperature and  $\delta^{18}\text{O}_{\text{water}}$  ranges corresponding to equilibrium precipitation of all the samples with oxygen isotope data (including quartz). Maximum burial depths for the northeast Dublin coast are poorly constrained owing to post-Carboniferous uplift, but vitrinite-reflectance and spore-color data from the central Dublin Basin suggest removal of 4.4–5.8 km of overburden (Fernandes and Clayton 2003). This would have produced a maximum burial temperature of 150 to  $200^\circ\text{C}$  with a nominal  $30^\circ\text{C}/\text{km}$  geothermal gradient and  $20^\circ\text{C}$  average surface temperature. Corresponding temperatures on the basin margin may have been lower. The host limestone data suggest that diagenetic alteration could have occurred in marine pore fluids during shallow to intermediate burial ( $\sim 20$  to  $100^\circ\text{C}$ ). While Figure 14D appears to show that all the calcite, dolomite, and quartz-cement  $\delta^{18}\text{O}$  values are compatible with a marine pore-fluid parentage within the estimated burial depths of the strata, the fluid-inclusion data (Fig. 13A, B) show that much higher fluid temperatures are required to account for the full range of calcite vein and vug, and quartz vein cements. It follows that many of the parent fluids must have been  $^{18}\text{O}$ -enriched relative to seawater.

Absolute  $\delta^{18}\text{O}_{\text{water}}$  values (VSMOW) for the fluids that precipitated quartz and calcite cements with both fluid-inclusion and  $\delta^{18}\text{O}_{\text{mineral}}$  data were calculated using equilibrium fractionation equations of Knauth and Epstein (1976) for quartz–water, of O’Neil et al. (1969) for calcite–water, and Sheppard and Schwarz (1970) for dolomite–water, with temperatures based on populations of  $T_h$  values from these cements. Five Tournaisian-hosted calcite vug and vein cements at Howth and Malahide yield a wide range in  $\delta^{18}\text{O}_{\text{water}}$  of  $-0.4$  to  $+20.4\text{‰}$  for temperatures between  $85$ – $283^\circ\text{C}$  (Fig. 15; Table S1). Ranges for individual samples are tighter, but almost all the calculated  $\delta^{18}\text{O}_{\text{water}}$  values are more positive than seawater ( $> 0\text{‰}$ ), and there is no clear stratigraphic or geographic pattern in the results. Higher temperatures correspond to more positive  $\delta^{18}\text{O}_{\text{water}}$  values, a pattern that cannot be explained by temperature-dependent O isotope

fractionation during calcite precipitation. The large range in  $\delta^{18}\text{O}$  values confirms that a single end-member water did not precipitate the calcites.

Three Viséan-hosted quartz veins yield a  $\delta^{18}\text{O}_{\text{water}}$  range of  $-9.5$  to  $+11.2\%$  for temperatures between  $105$  and  $333^\circ\text{C}$  (Fig. 15), higher temperatures again corresponding to more positive  $\delta^{18}\text{O}_{\text{water}}$  values (Table S1). As with the calcite cements, the wide range in  $\delta^{18}\text{O}_{\text{water}}$  values negates a single end-member water for quartz precipitation. In more detail, the zoned-CL vein-quartz sample from the Loughshinny Formation precipitated at higher temperatures ( $167$  to  $310^\circ\text{C}$ ) and from more  $^{18}\text{O}$ -enriched waters ( $+3.3$  to  $+10.2\%$ ) than the subsequent yellowish-brown CL quartz sample ( $60$  to  $156^\circ\text{C}$  and  $-9.5$  to  $+1.6\%$ ). The massive non-CL quartz sample from the Holmpatrick Formation records similar high temperatures and  $^{18}\text{O}$ -enriched fluids to the zoned quartz ( $151$  to  $333^\circ\text{C}$  and  $+2.4$  to  $+11.2\%$ ).

**Water–Rock Interaction.**—Oxygen isotope results from vein and vug cements record isotopic differences in the fluid source regions, overprinted by variable degrees of equilibration between fluids and the Mississippian limestones that host the vein and vug cements. This likely reflects a range of effective water:rock ratios, for example higher ratios (and/or a lack of reaction) where fluids were focused along fault-fracture conduits compared to lower ratios (and/or more substantial interaction) accompanying more dispersed or slower flow through pores in the carbonate rocks (Shelton et al. 2011; Hendry et al. 2015; Mohammadi et al. 2019a, 2019b). To investigate whether fluids isotopically equilibrated with the host rocks at the time of precipitation or imposed some of their “exotic” source characteristics,  $\delta^{18}\text{O}_{\text{water}}$  values that would be in equilibrium with adjacent or nearby host rocks were calculated for the same temperatures recorded in the cements for which both  $T_h$  and  $\delta^{18}\text{O}_{\text{mineral}}$  data are available (Fig. 15; Table S1). Results include examples of substantial host-rock equilibration (differences in  $\delta^{18}\text{O}_{\text{water}}$  values  $\leq 0.2\%$  for Tournaisian Feltrim Formation vug calcite and Tober Colleen Formation vein calcite) to minor equilibration ( $> 6\%$  disparity in  $\delta^{18}\text{O}_{\text{water}}$  values for Tournaisian Feltrim Formation vein calcite and Viséan Holmpatrick Formation vein quartz). The assumption here is that the rocks close to the veins were more likely to have interacted with the allochthonous vein-cementing fluids, albeit probably in a manner that is difficult to discern petrographically from the available sample set (e.g., selective replacement of matrix or subtle pore-filling cementation rather than wholesale replacement with significant textural changes). Such interaction is a likely consequence of residual porosity and permeability in the host syn-rift limestones that had not been subject to burial diagenesis, whereas calcite in dilatational veins cutting already lithified limestones may show much less fluid–rock interaction (e.g., Travé et al. 1998). Alternatively, it may reflect an early stage of dispersed fracturing or fault-tip propagation when flow is more diffused through a developing damage zone and the effective water:rock ratio is higher than when a more continuous but confined hydrological conduit is established (e.g., Benedicto et al. 2008; Baquès et al. 2010; Arndt et al. 2015).

Oxygen isotope data also reflect differences in lithologies encountered along regional flow paths. This is apparent from the wide range of elevated Sr isotope values shown in Figure 14B and Table 3, especially low- $\delta^{18}\text{O}$  vein cements with  $^{87}\text{Sr}/^{86}\text{Sr} > 0.7095$ . These are considerably more radiogenic than Mississippian seawater, as recorded in primary marine calcites (Mii et al. 1999) and require some fluids to have interacted with felsic siliciclastic or igneous rocks in order to assimilate radiogenic Sr (Douthit et al. 1993; McArthur et al. 2001). This interaction may also have influenced the fluid  $\delta^{18}\text{O}$  value, but much less than the  $^{87}\text{Sr}/^{86}\text{Sr}$  based on mass-balance considerations. In any case, the lack of a clear trend in Figure 14B indicates that other factors (e.g., temperature, fluid mixing, host limestone interaction) were more important in governing the cement oxygen isotope values. A single late-stage calcite vein from Loughshinny has a low  $^{87}\text{Sr}/^{86}\text{Sr}$  value (0.70828) that could indicate equilibration with

Mississippian limestones, but the  $\delta^{18}\text{O}$  value is much lower ( $-14.6\%$ ) than that of the adjacent limestone ( $-9.6\%$ ). Contrarily, one host limestone sample from close to the Carrickhill Fault at Malahide has an atypically high  $^{87}\text{Sr}/^{86}\text{Sr}$  value (0.70882). In this case contamination of the sample by diagenetic cement is the likely cause.

Oxygen isotope results for the dolomitized limestones, saddle dolomite cements in vugs, and zebra dolomite cements are equivocal in the absence of any viable fluid-inclusion data. Host-dolomite  $\delta^{18}\text{O}$  values can be explained by precipitation from warm marine pore fluids during burial (Fig. 14D), but the general paragenetic context of dolomite cement (Fig. 12) suggests formation at elevated temperatures from evolved pore fluids. For example, dolomite fringing a quartz vein at the Coppermine Fault has a  $\delta^{18}\text{O}$  value of  $-10.8\%$  (LSH-6A, Table 3). Early quartz cement adjacent to the fault has  $T_h$  values  $\geq 148^\circ\text{C}$ . If dolomite formed at similar temperatures, the pore fluids would have had  $\delta^{18}\text{O}$  values of  $\sim +2$  to  $+9\%$  VSMOW (Fig. 14D). A dolomitized clast in the Drumanagh Member debrite (LSH-7A; Table 3) was presumably altered before its reworking from the Balbriggan Block in the early Brigantian, and thus at shallow burial. Its  $\delta^{18}\text{O}$  value of  $-10.4\%$  is most realistically explained by hot, marine or higher-salinity pore fluids (e.g.,  $\sim 90^\circ\text{C}$  for marine pore fluid of  $-1\%$  VSMOW). Saddle morphology in dolomite cements is typically associated with precipitation temperatures  $> 60^\circ\text{C}$  (Radke and Mathis 1980; Gregg and Sibley 1984). Moreover, radiogenic  $^{87}\text{Sr}/^{86}\text{Sr}$  and negative  $\delta^{18}\text{O}$  values of dolomites and dolomite cements relative to limestones (Fig. 14A, B), imply that fault-related dolomitizing fluids retained geochemical signatures that were acquired in distal regions and imposed their signatures on the local rocks during dolomitization, as has been demonstrated for similar fault-related dolomitization in Mississippian rocks of the Isle of Man (Hendry et al. 2015).

Where oxygen isotope equilibration between cement-precipitating fluids and host limestones is recorded (e.g., Howth vug calcite and Malahide vein calcite, Fig. 15), the  $\delta^{13}\text{C}$  values of the cements are within  $1\%$  of host rock values (Tables 3, 4). Similarity in  $\delta^{13}\text{C}$  values is also noted for many vein calcites in which there is significant  $\delta^{18}\text{O}$  disequilibrium with respect to host rocks (Tables 3, S2). It is unsurprising that carbon isotope equilibrium was approached more effectively than oxygen isotope equilibrium given the water:rock ratio and mass-balance effects of a large carbon reservoir in the host rock compared to that of the fluid (Shelton 1983). However, atypically low  $\delta^{13}\text{C}$  values ( $-3.5$  to  $-7.6\%$ ) are recorded from samples H-1, H-3A, and H9A proximal to the HFF. These do not occur in the other samples from Howth, either those also close to the HFF, those displaying marked  $\delta^{18}\text{O}$  disequilibrium, or even some cements from the same hand specimens (Table 3). This suggests that these low  $\delta^{13}\text{C}$  values are not related to the fluid system but might instead be a residual primary or early diagenetic feature such as an imprint of syndepositional meteoric diagenesis. The current data set is inconclusive, and more detailed diagenetic study may be required to resolve this.

#### FLUID HISTORY, TECTONIC SETTING, AGE, AND CONCEPTUAL MODEL OF NORTH DUBLIN COAST DIAGENETIC MINERALIZATION

**Fluid History.**—Fluid-inclusion and stable-isotope data, guided by petrography, show a complex fluid history in the northeastern margin of the Dublin Basin, with multiple fluids and varying degrees of interaction among them and with strata through which they passed. This resulted in a range of calcite and dolomite compositions that is neither geographically nor stratigraphically correlated. Fluid inclusions from veins in Tournaisian and Viséan strata both document a high-salinity–low-temperature brine, which variably mixed with lower-salinity hydrothermal fluids (Fig. 13A–C). The latter appear to have been associated with individual fault systems along which localized Cu-sulfide and quartz mineralization could develop.

Oxygen isotope characterization of end-member fluids that interacted with the Mississippian limestones of the northeastern Dublin Basin is

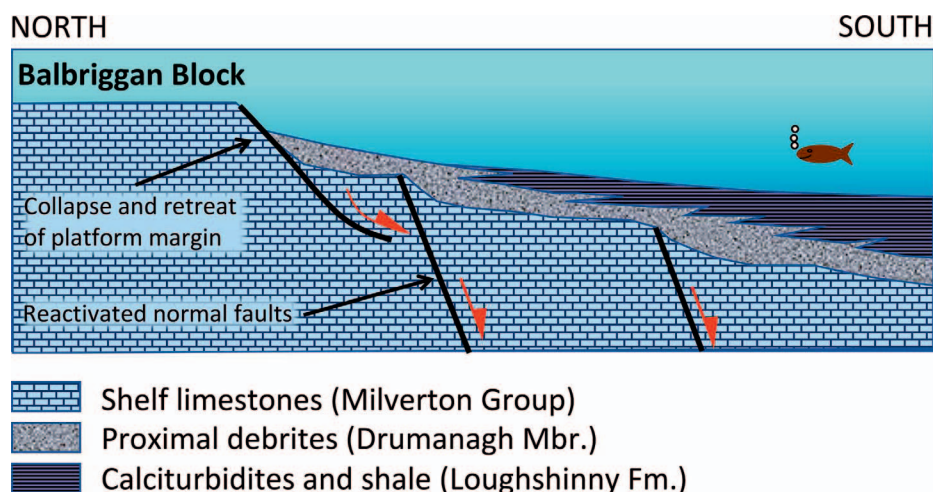


FIG. 16.—Cartoon showing the depositional context of the Drumanagh Member during earliest Brigantian collapse of the southern margin of the Balbriggan Block; presence of zebra-dolomite clasts in the debrite deposit implies hydrothermal dolomitization no later than early Brigantian and probably at shallow burial. Modified from Pickard et al. (1994).

complicated by the effect of water–rock interaction with diverse strata. Many of the fluids were highly evolved with respect to seawater by the time they precipitated cements on the basin margin (Fig. 15), and many had elevated salinities relative to seawater (up to  $8\times$  higher; Fig. 13A, B), but the data do not show a clear relationship between fluid-inclusion salinity and calculated  $\delta^{18}\text{O}_{\text{water}}$  value. Strontium isotope data (Fig. 14B) show that some fluids interacted with felsic silicates, but such interaction is unlikely to have enriched the water in  $^{18}\text{O}$  to very high values, given that such minerals are unlikely to have  $\delta^{18}\text{O}$  values  $> +8.5\text{‰}$  VSMOW (e.g., Bucholz et al. 2017, and references therein). Another possibility for high salinities and high  $\delta^{18}\text{O}_{\text{water}}$  values is that evaporated seawater contributed to the fluid system, as has been proposed for regional dolomitization and localized base-metal mineralization in the eastern Dublin Basin and Irish Midlands.

As previously noted, the three fluid end members of this study interpreted in Figure 13C resemble those observed by Gregg et al. (2001) and Johnson et al. (2009). The lower-temperature–higher-salinity “pervasive brine” corresponds to regional Fluid Type 1 of these authors, ascribed either to residual brine from seawater evaporation on extensive early Viséan carbonate platforms, and/or to brine that had dissolved Viséan peritidal evaporites (Banks et al. 2002), such as those around the Leinster Massif immediately south of the Dublin Basin (Nagy et al. 2004, 2005a, 2005b). These brines would have percolated into the basin by density reflux, displacing less dense formation fluids. The distinct high-temperature ( $T_h = 200$  to  $275^\circ\text{C}$ )–high-salinity brine trapped in Tournaisian-hosted calcite veins adjacent to the North and Carrickhill faults at Malahide might represent a portion of the “pervasive brine” that was entrained and heated in a higher-temperature fault-related system.

The “ore fluid” of Figure 13C resembles localized Fluid Type 3 of Johnson et al. (2009) (Fig. 13D). This brine interacted with underlying or fault-juxtaposed lower Paleozoic basement strata, either by density reflux or topographically driven flow, as the Variscan orogenic front migrated northwards (Garven et al. 1999), or by deep convection associated with elevated heat flow during syn-rift tectonism (Wilkinson et al. 2005). Such an augmented geothermal gradient may have driven deep seawater convection especially along extensional faults or at fault-intersection damage zones or dilatational jogs. These zones of structural complexity have widely been shown to be sites of massive dolomitization (e.g., Gomez-Rivas et al. 2014; Hollis et al. 2017) or to have provided fairways for later upward-moving dolomitizing fluids (e.g., Wilson et al. 2007; Iriarte et al. 2012). Our data set does not allow this fluid to be directly correlated with high  $^{87}\text{Sr}/^{86}\text{Sr}$  values, but its association with Cu-mineralized quartz veins strongly argues for basement involvement. The presence of Cu and apparent absence of Zn–Pb sulfides is at odds with the

Irish Midlands ore province and central Dublin Basin. This may indicate the relative importance of lower Paleozoic intermediate–mafic basement rocks along the basin margin (Williams et al. 1986; Breheny et al. 2016; Copage et al. 2017) compared to the influence of red-bed (Old Red Sandstone) metal source rocks in the Irish Midlands (Kinnaird et al. 2002). There may be thinner accumulations of red beds near the basin edge (e.g., Donabate Formation, Fig. 2) or alternatively, fault-related flow systems along the basin’s edge may have bypassed these rocks and tapped different basement metal source-rocks and fluid reservoirs.

The lower-salinity, lower-temperature regional Fluid Type 2 of the previous studies (Fig. 13D) is poorly represented in the north Dublin samples. Johnson et al. (2009) considered it to be a seawater-derived fluid that was unrelated to or did not encounter the conditions necessary for ore mineralization. Corresponding data from this study further suggest that it might be a product of cooling and mixing of the other two fluids (Fig. 13C). Notably, the only indication of fluids depleted in  $^{18}\text{O}$  relative to seawater is from later-stage quartz cement associated with the Coppermine Fault (Fig. 15). Meteoric waters may have locally recharged into the fluid circulation system during latest Chadian emergence and fluvial incision on the Balbriggan Block when the Smuggler’s Cove Formation was deposited (Fig. 2) or may have been transported up faults from the lower Paleozoic basement.

**Tectonic Setting and Age.**—Timing of fluid flow responsible for vein mineralization and fault-related dolomitization in the northeast Dublin Basin is not easy to constrain. Fault conduits were most likely active during extensional or transtensional tectonism, and multiple episodes of fluid flow cannot be ruled out. Faults most associated with veining and dolomitization are oriented NE–SW to E–W (Figs. 3, 5, 6). These are probably syn-rift faults following earlier Caledonian controls (Phillips and Sevastopoulou 1986; Johnston et al. 1996; Smit et al. 2018) that were later reactivated by Variscan compression, and potentially again during Mesozoic rifting in the offshore Irish Sea region (Kish Bank and Peel Basins). A potentially key piece of evidence for the timing of fault-related dolomitization comes from presumed hydrothermal zebra-dolomite clasts in the debrite facies of the Viséan Drumanagh Member at Loughshinny (Fig. 7G). These breccias were reworked from the eroding margin of the Milverton Group platform on the Balbriggan Block during the early Brigantian (Pickard et al. 1994) (Fig. 16), implying that the dolomite had already formed by that time. The dolomite probably precipitated at shallow burial depths from focused fluid flow, because no pre-Brigantian foraminifers are identified in the Drumanagh Member and deep incision of the Balbriggan Block is unlikely to have occurred.



dolomites postdating stylolites, Juerges et al. (2016) suggested that mineralization of the North Wales Platform most likely resulted from expulsion of basinal fluids during Variscan deformation. The interpretation was supported by studies of the Derbyshire–East Midlands Platform in the Pennines, where dolomitization and the emplacement of fluorite, barite, and galena have been linked to expulsion during Variscan compression of metalliferous brines from mudrocks in adjacent restricted hanging-wall basins (Frazer et al. 2014; Breislin 2018).

On the Isle of Man, an early Mesozoic age was favored for hydrothermal, fault-related dolomitization and Zn–Pb ore mineralization in Mississippian limestones (Shelton et al. 2011; Hendry et al. 2015). This was based on fault orientations and paleomagnetic data in co-occurring hematite, and such an age would have permitted Permo-Triassic strata in the East Irish Sea Basin to supply the evaporated seawater recorded as high fluid-inclusion salinities. However, no regional thermal anomaly has otherwise been recorded for this interval, and Hendry et al. (2015) noted that a late Viséan age remained a possibility, given that Tournaisian evaporites are present in adjacent basins and that Viséan volcanic rocks on the Isle of Man provide *prima facie* evidence of a period of elevated heat flow. Both scenarios would have favored fluid circulation on the dominant NE–SW extensional fault trends, interpreted as reactivated Caledonian structures (Smit et al. 2018), and the same trend and parentage is shown by the HHF, the Malahide North Fault, and the Loughshinny Coppermine Fault. The low  $\delta^{18}\text{O}$  and high Sr isotope values of fault-related dolomite–calcite mineralization on the Isle of Man similar to those in this study, with comparable  $T_h$  and salinity ranges (up to 300°C and to  $\geq 25$  wt% NaCl equivalent), and the presence of distinctive CL-zoned quartz in both cases are further circumstantial evidence for similar conditions of diagenesis (Hendry et al. 2015). The presence of Zn rather than Cu mineralization on the Isle of Man may reflect the presence of more felsic basement metal source rocks (Shelton et al. 2011). If valid, the comparison with the Irish Midlands and the Isle of Man implies that similar Mississippian syn-rift paleohydrological conditions were active across a geographical extent of more than 250 km. Different fault conduits episodically hosted or tapped into different hydrothermal cells with different fluid mixtures.

#### WIDER IMPLICATIONS

Although there are numerous published accounts of hydrothermal fault-related dolomitization in the literature, these relate to a variety of plate-tectonic settings and of ages relative to the host strata (see Hendry et al. 2015 and below for examples). Likewise, calcite cementation associated with normal faulting of already well-lithified pre-rift carbonates is well documented (e.g., Benedicto et al. 2008; Breesch et al. 2009; Baqués et al. 2010; Arndt et al. 2015). In contrast, few papers specifically report the characteristics of diagenesis in syn-rift carbonate platforms associated with rift-related fluid flow. Tectonic controls on carbonate sedimentation in rift basins have been explored in detail by Cross and Bosence (2008) and Dorobek (2008), but both limit consideration of diagenesis to the effects of footwall emergence and meteoric karstification. The impact of faulting on creating and rejuvenating fluid flow pathways, and of heat flow on driving fluid circulation and catalyzing diagenetic reactions, have received very little attention.

Hollis et al. (2017) and Hirani et al. (2018) describe hydrothermal dolomitization of pre-rift Eocene limestones in the Gulf of Suez by convecting seawater during early Miocene rift tectonism. They infer a two-stage history where initial fluid circulation from buried faults into the limestones during the onset of rifting produced stratabound dolomitization, then later focusing of fluid flow in the master fault during rift climax, when it breached the seabed, formed crosscutting dolomite bodies. Mineralized fracture corridors on the periphery of the fault damage zone controlled lateral fluid flow and the extent of this later dolomitization away from the fault, alternately acting as conduits and seals in response to the strain

history. It is possible that a similar scenario accompanied syn-rift diagenesis in the northeast Dublin Basin, although more detailed analysis of the dolomite bodies will be required to verify this. Similarities include crosscutting, locally brecciated dolomite bodies, stratabound dolomites extending away from faults, mineralized veins crosscutting, and locally terminating massive dolomitization. Differences include the extent of basement interaction and variety of fluid types involved, as deep hydrothermal seawater circulation on specific fault conduits was imposed upon more regional paleohydrologies. The Gulf of Suez example lacked zebra dolomites; Hirani et al. (2018) suggested that this may be the product of overprinting during later compressional or strike-slip tectonics. However, reworked Brigantian zebra dolomite in the Drumanagh Member argues that these can form during syn-rift diagenesis, possibly in response to strain cycling accompanying active faulting (cf. Vandeginste et al. 2005), and they clearly predate onset of Variscan compression.

Arosi and Wilson (2015) described the diagenesis of an early Miocene syn-tectonic carbonate platform from Sulawesi, noting that a regional burial diagenetic pattern predominated with only rare and localized marine and meteoric diagenesis on faulted highs. Syn-rift tectonism was recorded in differential subsidence, faulting, fracturing, and calcite veining, but synsedimentary fault orientations (inherited from basement structures) were oblique to the main extensional trend and may not have “tapped into” any syn-rift fluid circulation systems. In contrast, fault-related dolomitization of Oligo-Miocene limestones from Kalimantan was shown to be caused by warm seawater convection associated with magmatic activity but in a demonstrably post-rift setting (Wilson et al. 2007).

Stratabound and fault-parallel dolomite bodies with zebra fabrics in Early Cretaceous syn-rift limestones of northern Spain formed from hydrothermal and hypersaline fluids that interacted with siliciclastic basement lithologies and were transmitted up faults, but during strike-slip tectonics, several million years after limestone deposition (López-Horgue et al. 2010; Dewit et al. 2014). A similar scenario of post-rift hydrothermal dolomitization, calcite cementation, and Pb–Zn mineralization by large-scale thermal convection and basement interaction is documented by Gomez-Rivas et al. (2014) and Martín-Martín et al. (2015) in Early Cretaceous syn-rift carbonates in eastern Spain. These and other examples contrast with the interpretation of this paper, where alteration of the syn-rift carbonates took place in broadly contemporaneous syn-rift paleohydrologies.

Dolomite, calcite, and quartz cements filling vugs, fractures, and breccias in Cambrian–Ordovician basinal carbonates and siliciclastic rocks are associated with dolomitization, petroleum migration, and sulfide mineralization in the Reelfoot Rift of the southern Midcontinent of North America (Keller et al. 2000). The fluid salinities and temperatures at which these cements were precipitated are similar to those studied here, as are the rock lithologies involved. Unlike the fluids in this study, fluids in the Reelfoot Rift appear to have had limited communication with the adjacent carbonate platforms and were restricted within individual fault blocks. The timing of the fluid movement in the Reelfoot Rift is problematic but may have been related to late Paleozoic tectonism associated with Ouachita orogenic activity to the south, long after the initial period of rifting, which occurred during the Neoproterozoic and Early Cambrian (Keller et al. 2000) although an earlier origin cannot be ruled out.

Calcite vein cements associated with syn-rift fluid flow have been described by Travé et al. (1998) in Mesozoic limestones from NE Spain, but in this case deposition and diagenesis of the limestones long predated the Neogene rifting, and the cements were precipitated from meteoric waters that underwent little subsurface fluid–rock interaction. The North Dublin coast example emphasizes that deeper-penetrating hydrothermal fluid systems associated with active rifting not only formed vein cements, but were able to exploit residual permeability in limestones that had yet to experience deep burial, for example causing dolomitization away from fault conduits. This is considered more likely than a control of mechanical

stratigraphy (e.g., Dewit et al. 2014), given that grainy beds of the Malahide, Lane, and Holmpatrick Formations tend to be preferentially replaced (a possible exception being dolomitization of the Feltrim Formation mud-mound facies close to the HHF).

In summary, we hypothesize that the North Dublin coast exposures of the northeast Dublin Basin provide a rare window into the relationship of syn-rift carbonate deposition and syn-rift hydrothermal diagenesis. The wide range of fluid compositions and temperatures may be a hallmark of the dynamic and heterogeneous paleohydrologies that accompany the combination of active tectonism, enhanced heat flow, interaction of shallow paleoaquifers with fault-hosted hydrothermal systems, and host facies that have yet to undergo deep burial cementation. Fully testing this will require more detailed structural and geochronological studies, but by relating the diagenetic history and fluid types to coeval examples in the Irish Midlands we can propose that long-range fluid flow in shallow subsurface paleoaquifers combined with seawater-fed hydrothermal convection cells localized on active faults produced the geographically and stratigraphically varied cement compositions. Mineralization was confined to veins or extended laterally away from fault conduits as stratabound dolomite bodies depending on the intrinsic permeability and fracturing characteristics of the host limestones. High-temperature fluid interaction with basement silicate lithologies permitted ore mineralization whilst interaction of hydrothermal fluids and hypersaline brines favored dolomitization, as has been determined for coeval strata on the Isle of Man (Hendry et al. 2015) and in other hydrothermal dolomite occurrences cited above.

Cementation of paleoaquifers during deep burial and waning of heat flow and fault activity would have terminated fluid circulation and related diagenesis in the post-rift setting. Rejuvenation of subsurface fluid flow and fault-related diagenesis under different tectonic regimes cannot be ruled out, and Variscan fault-related mineralization has been proposed for the regionally correlative North Wales (Juerges et al. 2016) and Derbyshire (Frazer et al. 2014) platforms (although Breislin [2018] has recently proposed a low-temperature geothermal origin for stratabound dolomite in grainy platform margin facies of the Derbyshire platform related to syn-rift igneous activity). Additional work may be needed to conclusively determine whether fault-related dolomitization and Zn-Pb mineralization of Mississippian syn-rift limestones on the Isle of Man is Viséan or early Mesozoic in age, but the similarity in fluid temperatures and salinities and structural trends to those of this study are compelling.

### CONCLUSIONS

A combination of field observations, petrography, fluid-inclusion microthermometry, and stable-isotope analysis has been used to investigate calcite, dolomite, and quartz-vein cements, and fault-related dolomitization, in Mississippian syn-rift carbonates of the northeast Dublin Basin. Placed in a regional context, the results suggest that mineralization occurred coeval with the Viséan extensional tectonic episode, as laterally up-dip-derived hypersaline brines interacted with hydrothermal convection cells located on specific faults. Some of these cells transported marine-derived fluids into Paleozoic basement. Complex combinations of fluid cooling, mixing, and interaction with rocks along their flow paths, as well as with host limestones of varying facies, resulted in a wide range of diagenetic mineralogies and compositions that display both stratigraphic and geographic variability. We propose that this is a rare example of syn-rift diagenesis recorded in syn-rift limestones, as opposed to more commonly documented post-rift diagenesis in analogous strata. Some key observations and deductions are:

1. Fault-related stratabound and crosscutting pervasive nonplanar dolomitization in both Tournaisian and Viséan strata, but with associated zoned saddle-dolomite cements showing distinct CL stratigraphies. These differ from regional-scale CL microstratigraphy

described for otherwise similar dolomite cements in Lower Carboniferous rocks throughout the Irish Midlands and Dublin Basin (Wright et al. 2001) (Fig. S1). Faults were exploited by a variety of chemically distinct fluids over time, leading to the distinct chemical zonation patterns.

2. Multiple sets of calcite veins and localized quartz veins with fluid inclusions recording mixing of two dominant fluid types, a low-temperature ( $T_h = 60$  to  $135^\circ\text{C}$ )–high-salinity brine, like that found throughout the Irish Midlands (“pervasive brine”) and a high-temperature ( $T_h = 150$  to  $300^\circ\text{C}$ )–low- to moderate-salinity brine, similar to fluids recorded from Zn-Pb deposits in coeval limestones of the central Dublin Basin, Irish Midlands, and the Isle of Man (“ore fluid”). Scatter in the fluid-inclusion data record cooling of the ore fluid and mixing with the pervasive brine, with local evidence of pervasive brine entrainment into a fault-related hydrothermal cell associated with the Carrickhill and North faults at Malahide.
3. A paragenetic trend of host limestone, dolomite, and calcite cement  $\delta^{18}\text{O}$  (VPDB) values of  $\sim -3$  toward  $-22\%$  and from  $\delta^{13}\text{C}$  (VPDB) values of  $+4$  toward  $-4\%$ . The  $\delta^{18}\text{O}$  values of calcite veins become more negative with decreasing  $T_h$  values of their fluid inclusions, negating the possibility of precipitation from a single fluid. Calculated equilibrium  $\delta^{18}\text{O}_{\text{water}}$  values for quartz and calcite cement vary from  $\sim -9$  to  $+20\%$  VSMOW (but mostly  $> 0\%$ ), with varying isotopic equilibrium between vein-depositing waters and local host carbonate rocks possibly indicating higher water/rock ratios (and/or a lack of reaction) along confined fault-related fluid pathways and lower water/rock ratios (and/or more extensive reaction) associated with more dispersed flow through fracture networks or pore systems of limestone host rocks.
4. Carbonate  $^{87}\text{Sr}/^{86}\text{Sr}$  values ranging from  $\sim 0.7080$  in host limestone toward  $\sim 0.7090$  in dolomites to values  $> 0.7105$  in subsequent calcite veins showing that fluids interacted to varying extents with radiogenic silicates along their flow paths, most likely in fault-hosted hydrothermal cells that penetrated lower Paleozoic basement. Low  $\delta^{18}\text{O}$ –high  $^{87}\text{Sr}/^{86}\text{Sr}$  fluids retained allochthonous geochemical signatures and imposed these on local carbonate rocks during fault-related dolomitization.
5. Similarity of fluid types with those previously reported from the Irish Midlands and central Dublin Basin ore deposits, relationship of hydrothermal mineralization to Mississippian E–NE-trending extensional faults, and presence of reworked zebra dolomites in Brigantian debrites eroded from a footwall high all argue for a Viséan age of mineralization. Similar fault-related mineralization and paleofluid types documented from Mississippian limestones on the Isle of Man (Shelton et al. 2011; Hendry et al. 2015) suggest that these might also be products of Viséan syn-rift diagenesis rather than early Mesozoic in age.
6. High-temperature fluids and basement rock involvement appears to have been a prerequisite for the ore mineralization, while mixing with high-salinity fluids in localized fault conduits favored hydrothermal dolomitization. Occurrence of Cu-sulfides and absence of Zn-Pb sulfides at the Coppermine Fault may reflect the relative importance of intermediate–mafic basement rocks in the extensional environment of the basin margin compared to red-bed sandstone metal source rocks of the Irish Midlands.

### SUPPLEMENTAL MATERIAL

Supplemental files are available from JSR's Data Archive.

### ACKNOWLEDGMENTS

Initial support for this study was provided by a grant from the J. William Fulbright Foreign Scholarship Board and the United States Information Agency

to J.M.G. We acknowledge support from Enterprise Ireland (Forbairt) to I.D.S., the National Science Foundation (U.S.A.) (NSF-INT-9729653 and NSF-EAR-0106388) to J.M.G. and K.L.S., and the donors of the Petroleum Research Fund, administered by the American Chemical Society (PRF 35893-AC8) to J.M.G. and K.L.S. Further support was provided by the John and Betty Marshall Opportunities for Excellence Fund and the Midas Ore Research Fund of the University of Missouri to K.L.S. We thank Tom Culligan (UCD) for preparation of petrographic samples. We thank Cathy Hollis and Colin Braithwaite, as well as Editors Steven Kaczmarek and Leslie Melim, for very detailed feedback on earlier iterations of our manuscript. Their challenges prompted us to re-focus our interpretations and draw greater significance from our data set, and so enabled us to substantially improve the final product. John Southard is thanked for helpful copy editing of the final manuscript.

## REFERENCES

- ARNDT, M., VIRGO, S., COX, S.F., AND URAI, J.L., 2015, Changes in fluid pathways in a calcite vein mesh (Natih Formation, Oman Mountains): insights from stable isotopes: *Geofluids*, v. 14, p. 391–418.
- AROSI, H.A., AND WILSON, M.E.J., 2015, Diagenesis and fracturing of a large-scale, syntectonic carbonate platform: *Sedimentary Geology*, v. 326, p. 109–124.
- BANKS, D.A., BOYCE, A.J., AND SAMSON, I.M., 2002, Constraints on the origins of fluids forming Irish Zn–Pb–Ba deposits: evidence from the composition of fluid inclusions: *Economic Geology*, v. 97, p. 471–480.
- BAQUÉS, V., TRAVÉ, A., BENEDICTO, A., LABAUME, P., AND CANTARERO, I., 2010, Relationships between carbonate fault rocks and fluid flow regime during propagation of the Neogene extensional faults of the Penedès basin (Catalan Coastal Ranges, NE Spain): *Journal of Geochemical Exploration*, v. 106, p. 24–33.
- BENEDICTO, A., PLAGNES, V., VERGÉLY, P., FLOTTÉ, N., AND SCHULTZ, R.A., 2008, Fault and fluid interaction in a rifted margin: integrated study of calcite-sealed fault-related structures (southern Corinth margin), in *Wibberley, C.A.J., Kurtz, W., Imber, J., Holdsworth, R.E., and Collettini, C., eds., The Internal Structure of Fault Zones: Implications for Mechanical and Fluid-Flow Properties: Geological Society of London, Special Publication 299*, p. 1–19.
- BLAKEMAN, R.J., ASHTON, J.H., BOYCE, A.J., FALLOCK, A.E., AND RUSSELL, M.J., 2002, Timing of interplay between hydrothermal and surface fluids in the Navan Zn + Pb orebody, Ireland: evidence from metal distribution trends, mineral textures, and  $\delta^{34}\text{S}$  analyses: *Economic Geology*, v. 97, p. 73–91.
- BODNAR, R.J., 1993, Revised equation and table for determining the freezing point depression of  $\text{H}_2\text{O}$ –NaCl solutions: *Geochimica et Cosmochimica Acta*: v. 57, p. 683–684.
- BODNAR, R.J., AND VITYK, M.O., 1994, Interpretation of microthermometric data for  $\text{H}_2\text{O}$ –NaCl fluid inclusions, in *De Vivo, B., and Frezzotti, M.L., eds., Fluid Inclusions in Minerals: Methods and Applications: Blacksburg, Virginia Polytechnic Institute and State University*, p. 117–130.
- BRAITHWAITE, C.J.R., AND RIZZI, G., 1997, The geometry and petrogenesis of hydrothermal dolomites at Navan, Ireland: *Sedimentology*, v. 44, p. 421–440.
- BREESCH, L., SWENNEN, R., AND VINCENT, B., 2009, Fluid flow reconstruction in hanging and footwall carbonates: compartmentalization by Cenozoic reverse faulting in the Northern Oman Mountains (UAE): *Marine and Petroleum Geology*, v. 26, p. 113–128.
- BREHENY, C., MOORE, K.R., COSTANZO, A., AND FEELY, M., 2016, Reconstruction of an Ordovician seafloor volcanohydrothermal system: a case study from the Copper Coast, southeastern Ireland using field, geochemical and fluid inclusion data: *Mineralogical Magazine*, v. 80, p. 157–184.
- BREISLIN, C.J., 2018, Basin-Scale Mineral and Fluid Processes at a Platform Margin, Lower Carboniferous, UK [PhD thesis]: University of Manchester, 236 p.
- BROWN, P.E., AND HAGEMANN, S.G., 1995, MacFlinCor and its application to fluids in Archean lode-gold deposits: *Geochimica et Cosmochimica Acta*, v. 19, p. 3943–3952.
- BUCHOLZ, C.E., JAGOUTZ, O., VAN TONGEREN, J.A., SETERA, J., AND WANG, Z., 2017, Oxygen isotope trajectories of crystallizing melts: insights from modeling and the plutonic record: *Geochimica et Cosmochimica Acta*, v. 207, p. 157–184.
- CLAYTON, R.N., AND MAYEDA, T.K., 1963, The use of bromine-pentafluoride in the extraction of oxygen from oxides and silicates for isotopic analyses: *Geochimica et Cosmochimica Acta*, v. 27, p. 43–52.
- COPAGE, J., MEERE, P., SOLFERINO, G., AND UNITT, R., 2017, The geochemistry of the Waterford Copper Coast mineralization, Ireland: *Applied Geoscience*, v. 126, p. 50–51.
- CORCORAN, D.V., AND CLAYTON, G., 2001, Interpretation of vitrinite reflectance profiles in sedimentary basins, onshore and offshore Ireland, in *Shannon, P.M., Haughton, P.W.D., and Corcoran, D.V., eds., The Petroleum Exploration of Ireland's Offshore Basins: Geological Society of London, Special Publication 188*, p. 61–90.
- CRAWFORD, M.L., 1981, Phase equilibria in aqueous fluid inclusions: *Mineralogical Association of Canada, Short Course Handbook 6*, p. 75–100.
- CROSS, N.E., AND BOSENCE, D.W.J., 2008, Tectono-sedimentary models for rift-basin carbonate systems, in *Lukasik, J., and Simo, J.A., eds., Controls on Carbonate Platform and Reef Development, SEPM, Special Publication 89*, p. 83–105.
- DAVIES, G.R., AND SMITH, L.B., 2006, Structurally controlled hydrothermal dolomite reservoir facies: an overview: *American Association of Petroleum Geologists, Bulletin*, v. 90, p. 1641–1690.
- DE BRIT, T.J., 1989, Timing structural events and base metal emplacement using extension veins and cements in the Carboniferous of North Central Ireland: *Irish Journal of Earth Sciences*, v. 10, p. 13–31.
- DEWIT, J., FOUBERT, A., EL DESOUKY, H.A., MUCHEZ, P., HUNT, D., VAN HAECKE, F., AND SWENNEN, R., 2014, Characteristics, genesis and parameters controlling the development of a large stratabound HTD body at Matienzo (Ramales Platform, Basque–Cantabrian Basin, northern Spain): *Marine and Petroleum Geology*, v. 55, p. 6–25.
- DIAMOND, L.W., 1992, Stability of  $\text{CO}_2$  clathrate hydrate +  $\text{CO}_2$  liquid +  $\text{CO}_2$  vapour + aqueous KCl–NaCl solutions: experimental determination and application to salinity estimates of fluid inclusions: *Geochimica et Cosmochimica Acta*, v. 56, p. 273–280.
- DICKSON, J.A.D., 1965, A modified staining technique for carbonates in thin section: *Nature*, v. 205, p. 587.
- DIXON, P.R., LEHURAY, A.P., AND RYE, D.M., 1987, Pb isotopic evidence for basement structure and composition in Central Ireland: *Geological Society of America, Abstracts with Programs*, v. 19, p. 644.
- DOROBOK, S.L., 2008, Tectonic and depositional controls on syn-rift carbonate platform sedimentation, in *Lukasik, J., and Simo, J.A., eds., Controls on Carbonate Platform and Reef Development: SEPM, Special Publication 89*, p. 57–81.
- DOUTHIT, T.L., MEYERS, W.J., AND HANSON, G.N., 1993, Nonmonotonic variation of seawater  $^{87}\text{Sr}/^{86}\text{Sr}$  across the Ivorian/Chadian boundary (Mississippian, Osagean): evidence from marine cements within the Irish Waulsortian limestone: *Journal of Sedimentary Petrology*, v. 63, p. 539–549.
- FERNANDES, P., AND CLAYTON, G., 2003, Organic maturation levels and thermal history of the Carboniferous rocks of the Dublin Basin, in *Wong, T.E., ed., XVth International Congress of Carboniferous and Permian Stratigraphy, Proceedings: Utrecht, Royal Netherlands Academy of Arts and Sciences, 10–16 August*, p. 37–45.
- FOLK, R.L., 1965, Some Aspects of recrystallization in ancient limestones, in *Pray, L.C., and Murray, R.C., eds., Dolomitization and Limestone Diagenesis: SEPM, Special Publication 13*, p. 14–48.
- FRAZER, M., WHITAKER, F., AND HOLLIS, C., 2014, Fluid expulsion from overpressured basins: implications for Pb–Zn mineralisation and dolomitisation of the east Midlands platform, England: *Marine and Petroleum Geology*, v. 55, p. 68–86.
- GARVEN, G., APPOLD, M.S., TOPTYGINA, V.I., AND HAZLETT, T.J., 1999, Hydrogeologic modeling of the genesis of carbonate-hosted lead-zinc ores: *Hydrogeology Journal*, v. 7, p. 108–126.
- GAWTHORPE, R.L., GUTTERIDGE, P., AND LEEDER, M.R., 1988, Late Devonian and Dinantian basin evolution in northern England and Wales, in *Arthurton, R.S., Gutteridge, P., and Nolan, S.C., eds., The Role of Tectonics in Devonian and Carboniferous Sedimentation in the British Isles: Yorkshire Geological Society, Occasional Publication 6*, p. 1–23.
- GOLDSTEIN, R.H., AND REYNOLDS, T.J., 1994, Systematics of Fluid Inclusions in Diagenetic Minerals: *SEPM, Short Course 31*.
- GOMEZ-RIVAS, E., CORBELLA, M., MARTÍN-MARTÍN, J.D., STAFFORD, S.L., TEIXELL, A., BONS, P.D., GRIERA, A., AND CARDELLACH, E., 2014, Reactivity of dolomitizing fluids and Mg source evaluation of fault controlled dolomitization at the Benicàssim outcrop analogue (Maestrat basin, E Spain): *Marine and Petroleum Geology*, v. 55, p. 26–42.
- GREGG, J.M., AND SIBLEY, D.F., 1984, Epigenetic dolomitization and the origin of xenotopic dolomite texture: *Journal of Sedimentary Petrology*, v. 54, p. 908–931.
- GREGG, J.M., SHELTON, K.L., JOHNSON, A.W., SOMERVILLE, I.D., AND WRIGHT, W.R., 2001, Dolomitization of the Waulsortian limestone (Lower Carboniferous) in the Irish Midlands: *Sedimentology*, v. 48, p. 745–766.
- HARRISON, P.H., AND HENDERSON, K., 2004, Loughshinny base metal project: final and relinquishment report, Plates 3219 and 3220: *Irish Geological Survey*.
- HENDRY, J.P., GREGG, J.M., SHELTON, K.L., SOMERVILLE, I.D., AND CROWLEY, S.F., 2015, Origin, characteristics and distribution of fault- and fracture-related dolomitisation: insights from Lower Carboniferous carbonates, Isle of Man, UK: *Sedimentology*, v. 62, p. 717–752.
- HIRANI, J., BASTESEN, E., BOYCE, A., CORLETT, H., EKER, A., GAWTHORPE, R., HOLLIS, C., KORNEVA, I., AND ROTEVATN, S., 2018, Structural controls on non fabric-selective dolomitization within rift-related basin-bounding normal fault systems: insights from the Hammam Farauq Fault, Gulf of Suez, Egypt: *Basin Research*, v. 30, p. 990–1014.
- HITZMAN, M.W., AND BEATY, D.W., 1996, The Irish Zn–Pb–(Ba) orefield, in *Sangster, D.F., ed., Carbonate-Hosted Lead-Zinc Deposit: Society of Economic Geologists, Special Publication 4*, p. 112–143.
- HITZMAN, M.W., ALLEN, J.R., AND BEATY, D.W., 1998, Regional dolomitization of the Waulsortian limestone in southeastern Ireland: evidence of large-scale fluid flow driven by the Hercynian orogeny: *Geology*, v. 26, p. 547–550.
- HOLLIS, C., BASTESEN, E., BOYCE, A., CORLETT, H., GAWTHORPE, R., HIRANI, J., ROTEVATN, A., AND WHITAKER, F., 2017, Fault-controlled dolomitization in a rift basin: *Geology*, v. 45, p. 219–222.
- HORITA, J., 2014, Oxygen and carbon isotope fractionation in the system dolomite–water– $\text{CO}_2$  at elevated temperatures: *Geochimica et Cosmochimica Acta*, v. 129, p. 111–124.
- IRIARTE, E., LÓPEZ-HORGUE, M.A., SCHROEDER, S., AND CALINE, B., 2012, Interplay between fracturing and hydrothermal fluid flow in the Asón Valley hydrothermal dolomites (Basque–Cantabrian Basin, Spain), in *Garland, J., Neilson, J.E., Laubach, S.E., and Whidden, K.J., eds., Advances in Carbonate Exploration and Reservoir Analysis: Geological Society of London, Special Publication 370*, p. 207–227.

- JONES, G.L., SOMERVILLE, I.D., AND STROGEN, P., 1988, The Lower Carboniferous (Dinantian) of the Swords area: sedimentation and tectonics in the Dublin basin, Ireland: *Geological Journal*, v. 23, p. 221–248.
- JOHNSON, A.W., SHELTON, K.L., GREGG, J.M., SOMERVILLE, I.D., WRIGHT, W.R., AND NAGY, Z.R., 2009, Regional studies of dolomites and their included fluids: recognizing multiple chemically distinct fluids during the complex diagenetic history of Lower Carboniferous (Mississippian) rocks of the Irish Zn-Pb ore field: *Mineralogy and Petrology*, v. 96, p. 1–18.
- JOHNSTON, J.D., 1999, Regional fluid flow and the genesis of Irish Carboniferous base metal deposits: *Mineralium Deposita*, v. 34, p. 571–598.
- JOHNSTON, J., COLLIER, D., MILLAR, G., AND CRITCHLEY, M.F., 1996, Basement structural controls on Carboniferous-hosted base metal mineral deposits in Ireland, in Strogon, P., Somerville, I.D., and Jones, G.L., eds., *Recent Advances in Lower Carboniferous Geology*: Geological Society of London, Special Publication 107, p. 1–21.
- JURGES, A., HOLLIS, C.E., MARSHALL, J., AND CROWLEY, S., 2016, The control of basin evolution on patterns of sedimentation and diagenesis: an example from the Mississippian Great Orme, North Wales: *Geological Society of London, Journal*, v. 173, p. 438–456.
- KELLER, T.J., GREGG, J.M., AND SHELTON, K.L., 2000, Fluid migration and associated diagenesis in the Greater Reelfoot rift region, Midcontinent, United States: *Geological Society of America, Bulletin*, v. 112, p. 1680–1693.
- KINNAIRD, J.A., IXER, R.A., BARREIRO, B., AND NEX, P.A.M., 2002, Contrasting sources for lead in Cu-polymetallic and Zn-Pb mineralization in Ireland: constraints from lead isotopes: *Mineralium Deposita*, v. 37, p. 495–511.
- KNAUTH, L.P., AND EPSTEIN, S., 1976, Hydrogen and oxygen isotope ratios in nodular and bedded cherts: *Geochimica et Cosmochimica Acta*, v. 40, p. 1095–1108.
- LAND, L.S., 1980, The isotopic and trace element geochemistry of dolomite: the state of the art, in Zenger, D.H., Dunham, J.B., and Ethington, R.L., eds., *Concepts and Models of Dolomitization*: SEPM, Special Publication 28, p. 87–110.
- LEES, A., AND MILLER, J., 1995, Waulsortian banks, in Monty, C.L.V., Bosence, D.W.J., Bridges, P.H., and Pratt, B.R., eds., *Carbonate Mud-Mounds, Their Origin and Evolution*: International Association of Sedimentologists, Special Publication 23, p. 191–271.
- LÓPEZ-HORGUE, M.A., IRIARTE, E., SCHRÖDER, S., FERNÁNDEZ-MENDIOLA, P.A., CALINE, B., CORNEILLIE, H., FRÉMONT, J., SUDRIE, M., AND ZERTI, S., 2010, Structurally controlled hydrothermal dolomites in Albian carbonates of the Ason Valley, Basque Cantabrian Basin, Northern Spain: *Marine and Petroleum Geology*, v. 27, p. 1069–1092.
- MACDERMOT, C.V., AND SEVASTOPOULO, G.D., 1972, Upper Devonian and Lower Carboniferous stratigraphical setting of Irish mineralization: *Geological Survey of Ireland, Bulletin*, v. 1, p. 267–280.
- MARCHANT, T.R., 1978, The stratigraphy and micropaleontology of the Lower Carboniferous (Courseyan–Arundian) of the Dublin basin, Ireland [PhD thesis]: Trinity College, Dublin, 420 p.
- MARTÍN-MARTÍN, J.D., TRAVÉ, A., GÓMEZ-RIVAS, E., SALAS, R., SIZUN, J.-P., VERGÉS, J., CORBELLA, M., STAFFORD, S.L., AND ALFONSO, P., 2015, Fault-controlled and stratabound dolostones in the late Aptian–earliest Albian Benassal Formation (Maestrat Basin, E Spain): petrology and geochemistry constrains: *Marine and Petroleum Geology*, v. 65, p. 83–102.
- MATLEY, C.S., AND VAUGHAN, A., 1908, The Carboniferous rocks at Loughshinny (County Dublin): *Geological Society of London, Quarterly Journal*, v. 64, p. 413–474.
- MCCARTHUR, J.M., DONOVAN, D.T., THIRLWALL, M.F., FOLKE, B.W., AND MATTEY, D., 2000, Strontium isotope profile of the early Toarcian (Jurassic) oceanic anoxic event, the duration of ammonite biozones, and belemnite palaeotemperatures: *Earth and Planetary Science Letters*, v. 179, p. 269–285.
- MCCARTHUR, J.M., HOWARTH, R.J., AND BAILEY, T.R., 2001, Strontium isotope stratigraphy: LOWESS version 3: best fit to the marine Sr isotope curve for 0–509 Ma and accompanying look-up table for deriving numerical age: *Journal of Geology*, v. 109, p. 155–170.
- MCCONNELL, B., PHILCOX, M.E., MACDERMOT, C.V., AND SLEEMAN, A.G., 1995, *Geology of Kildare–Wicklow*: Geological Survey of Ireland, Sheet 16, 1:100,000 scale.
- MIL, H., GROSSMAN, E.L., AND YANCEY, T.E., 1999, Carboniferous isotope stratigraphies of North America: implications for carboniferous paleoceanography and Mississippian glaciation: *Geological Society of America, Bulletin*, v. 111, p. 960–973.
- MOHAMMADI, S., EWALD, T.A., GREGG, J.M., AND SHELTON, K.L., 2019a, Diagenesis of Mississippian carbonate rocks in north-central Oklahoma, USA, in Grammer, G.M., Gregg, J.M., Puckette, J.O., Jaiswal, P., Mazzullo, S.J., Pranter, M.J., and Goldstein, R.H., eds., *Mississippian Reservoirs of the Midcontinent*: American Association of Petroleum Geologists, Memoir 116. doi:10.1306/13632153M1163791
- MOHAMMADI, S., GREGG, J.M., SHELTON, K.L., APPOLD, M.S., AND PUCKETTE, J.O., 2019b, Influence of late diagenetic fluids on Mississippian carbonate rocks on the Cherokee–Ozark Platform, NE Oklahoma, NW Arkansas, SW Missouri, SE Kansas, in Grammer, G.M., Gregg, J.M., Puckette, J.O., Jaiswal, P., Mazzullo, S.J., Pranter, M.J., and Goldstein, R.H., eds., *Mississippian Reservoirs of the Midcontinent*: American Association of Petroleum Geologists, Memoir 116. doi:10.1306/13632154M1163791
- MUR-WOOD, R.M., 1994, Earthquakes, strain-cycling and the mobilization of fluids, in Parnell, J., ed., *Geofluids: Origin, Migration and Evolution of Fluids in Sedimentary Basins*: Geological Society of London, Special Publication 78, p. 85–98.
- NAGY, Z.R., GREGG, J.M., SHELTON, K.L., BECKER, S.P., SOMERVILLE, I.D., AND JOHNSON, A.W., 2004, Early dolomitisation and fluid migration through the Lower Carboniferous carbonate platform in the southeast Irish Midlands: implications for reservoir attributes, in Braithwaite, C., Rizzi, G., and Darke, G., eds., *The Geometry and Petrogenesis of Dolomite Hydrocarbon Reservoirs*: Geological Society of London, Special Publication 235, p. 367–392.
- NAGY, Z.R., SOMERVILLE, I.D., GREGG, J.M., BECKER, S.P., AND SHELTON, K.L., 2005a, Sedimentology and stratigraphy of Upper Tournaian–Viséan (Mississippian, Lower Carboniferous) carbonate rocks in south Co. Wexford, Ireland: an example of sedimentation in an actively tilting basin: *Sedimentology*, v. 52, p. 489–512.
- NAGY, Z.R., SOMERVILLE, I.D., GREGG, J.M., BECKER, S.P., AND SHELTON, K.L., 2005b, Lower Carboniferous peritidal carbonates and associated evaporites adjacent to the Leinster Massif, southeast Irish Midlands: *Geological Journal*, v. 40, p. 173–192.
- NEWMAN, P.J., 1999, The geology and hydrocarbon potential of the Peel and Solway basins, East Irish Sea: *Journal of Petroleum Geology*, v. 22, p. 305–324.
- NOLAN, S.C., 1986, *The Carboniferous geology of the Dublin area* [PhD thesis]: Trinity College, Dublin, 319 p.
- NOLAN, S.C., 1989, The style and timing of Dinantian syn-sedimentary tectonics in the eastern part of the Dublin basin, Ireland, in Arthurton, R.S., Gutteridge, P., and Nolan, S.C., eds., *The Role of Tectonics and Carboniferous Sedimentation in the British Isles*: Yorkshire Geological Society, Occasional Publication 6, p. 83–97.
- O'HARA, K.D., 1995, A note on the structural and fluid inclusion characteristics of quartz veins at Howth, County Dublin: *Irish Journal of Earth Sciences*, v. 14, p. 59–64.
- O'NEIL, J.R., CLAYTON, R.N., AND MAYEDA, T.K., 1969, Oxygen isotope fractionation in divalent metal carbonates: *Journal of Chemical Physics*, v. 51, p. 5547–5558.
- PHILCOX, M., JONES, G.L., SOMERVILLE, I.D., AND STROGEN, P., 1995, The Carboniferous limestone of the North Dublin coast and Feltrim Hill, in *Irish Carbonate-Hosted Zn-Pb Deposits*: Society of Economic Geologists, Guidebook Series 21, p. 173–208.
- PHILLIPS, W.E.A., AND SEVASTOPOULO, G.D., 1986, The stratigraphic and structural setting of Irish mineral deposits, in Andrew, C.J., Crowe, R.W.A., Finlay, S., Pennell, W.M., and Pyne, J.F., eds., *Geology and Genesis of Mineral Deposits in Ireland*: Dublin, Irish Association for Economic Geology, p. 1–30.
- PICKARD, N.A.H., REES, J.R., STROGEN, P., SOMERVILLE, I.D., AND JONES, G.L., 1994, Controls on the evolution and demise of late Dinantian carbonate platforms, northern margin of the Dublin Basin, Ireland: *Geological Journal*, v. 9, p. 93–117.
- RADKE, B.M., AND MATHIS, R.L., 1980, On the formation and occurrence of saddle dolomites: *Journal of Sedimentary Petrology*, v. 50, p. 1149–1168.
- REES, J.C., 1987, *The Carboniferous geology of the Boyne Valley area, Ireland* [PhD thesis]: Trinity College, Dublin, 374 p.
- ROEDDER, E., 1984, Fluid Inclusions: *Mineralogical Society of America, Reviews in Mineralogy*, v. 12, 646 p.
- ROSENBAUM, J., AND SHEPPARD, S.M.F., 1986, An isotopic study of siderites, dolomites and ankerites at high temperatures: *Geochimica et Cosmochimica Acta*, v. 50, p. 1147–1150.
- RUSSELL, M.J., 1978, Downward-excavating hydrothermal cells and Irish-type ore deposits: importance of an underlying thick Caledonian prism: *Institute of Mining and Metallurgy, Transactions*, v. 87, p. 168–171.
- RUSSELL, M.J., 1986, Extension and convection: a genetic model for the Irish Carboniferous base-metal and barite deposits, in Andrew, C.J., Crowe, R.W.A., Finlay, S., Pennell, W.M., and Pyne, J.F., eds., *Geology and Genesis of Mineral Deposits in Ireland*: Dublin, Irish Association for Economic Geology, p. 545–554.
- SEVASTOPOULO, G.D., AND WYSE JACKSON, P.N., 2009, Chapter 10. Carboniferous: Mississippian (Tournaisian and Viséan), in Holland, C.H., and Saunders, I., eds., *The Geology of Ireland*, 2nd Edition: Edinburgh, Dunedin Academic Press, p. 215–268.
- SHELTON, K.L., 1983, Composition and origin of ore-forming fluids in a carbonate-hosted porphyry copper and skarn deposit: a fluid inclusion and stable isotope study of Mines Gaspé, Quebec: *Economic Geology*, v. 78, p. 387–421.
- SHELTON, K.L., AND ORVILLE, P.M., 1980, Formation of synthetic fluid inclusions in natural quartz: *American Mineralogist*, v. 65, p. 1233–1236.
- SHELTON, K.L., GREGG, J.M., AND JOHNSON, A.W., 2009, Replacement dolomites and ore sulfides as recorders of multiple fluids and fluid sources in the southeast Missouri MVT district, USA: halogen–<sup>87</sup>Sr/<sup>86</sup>Sr–<sup>δ</sup>18O–<sup>δ</sup>34S systematics in the Bonnetterre Dolomite: *Economic Geology*, v. 104, p. 733–748.
- SHELTON, K.L., BEASLEY, J.M., GREGG, J.M., APPOLD, M.S., CROWLEY, S.F., HENDRY, J.P., AND SOMERVILLE, I.D., 2011, Evolution of a Carboniferous carbonate-hosted sphalerite breccia deposit, Isle of Man: *Mineralium Deposita*, v. 46, p. 859–880.
- SHEPPARD, S.M.F., AND SCHWARZ, H.P., 1970, Fractionation of carbon and oxygen isotopes and magnesium between coexisting metamorphic calcite and dolomite: *Contributions to Mineralogy and Petrology*, v. 26, p. 161–198.
- SIBLEY, D.F., AND GREGG, J.M., 1987, Classification of dolomite textures: *Journal of Sedimentary Petrology*, v. 57, p. 967–975.
- SIBSON, R.H., 1994, Crustal stress, faulting and fluid flow, in Parnell, J., ed., *Geofluids: Origin, Migration and Evolution of Fluids in Sedimentary Basins*: Geological Society of London, Special Publication 78, p. 69–84.
- SMIT, J., VAN WEES, J.-D., AND CLOETINGH, S., 2018, Early Carboniferous extension in East Avalonia: 350 My record of lithospheric memory: *Marine and Petroleum Geology*, v. 92, p. 1010–1027.
- SOMERVILLE, I.D., 2003, Review of Irish Lower Carboniferous (Mississippian) mud-mounds: depositional setting, biota, facies and evolution, in Ahr, W., Harris, A.P., Morgan, W.A., and Somerville, I.D., eds., *Permo-Carboniferous Carbonate Platforms and Reefs*: SEPM, Special Publication 78, and American Association of Petroleum Geologists, Memoir 83, p. 239–252.

- SOMERVILLE, I.D., PICKARD, A.H., STROGEN, P., AND JONES, G.L., 1992a, Early to mid-Viséan shallow water platform buildups, north Co. Dublin, Ireland: *Geological Journal*, v. 27, p. 151–172.
- SOMERVILLE, I.D., STROGEN, P., AND JONES, G.L., 1992b, Mid-Dinantian Waulsortian buildups in the Dublin Basin, Ireland: *Sedimentary Geology*, v. 79, p. 91–116.
- SOMERVILLE, I.D., AND WATERS, C.N., 2011, Chapter 21. Dublin Basin. A Revised Correlation of Carboniferous Rocks in the British Isles: Geological Society of London, Special Report 26, p. 138–143.
- STROGEN, P., JONES, G.L., AND SOMERVILLE, I.D., 1990, Stratigraphy and sedimentology of Lower Carboniferous (Dinantian) boreholes from west Co. Meath, Ireland: *Geological Journal*, v. 25, p. 103–137.
- STROGEN, P., SOMERVILLE, I.D., PICKARD, N.A.H., JONES, G.L., AND FLEMING, M., 1996, Controls on ramp, platform and basinal sedimentation in the Dinantian of the Dublin Basin and Shannon Trough, Ireland, in Strogen, P., Somerville, I.D., and Jones, G.L., eds., *Recent Advances in Lower Carboniferous Geology*: Geological Society of London, Special Publication 107, p. 263–279.
- TRAVÉ, A., CALVET, F., SOLER, A., AND LABAUME, P., 1998, Fracturing and fluid migration during Palaeogene compression and Neogene extension in the Catalan Coastal Ranges, Spain: *Sedimentology*, v. 45, p. 1063–1082.
- VANDEGINSTE, V., SWENNEN, R., GLEESON, S.A., ELLAM, R.M., OSADETZ, K., AND ROURE, F., 2005, Zebra dolomitization as a result of focused fluid flow in the Rocky Mountains Fold and Thrust Belt, Canada: *Sedimentology*, v. 52, p. 1067–1095.
- WILKINSON, J.J., 2003, On diagenesis, dolomitisation and mineralisation in the Irish-type Zn-Pb Orefield: *Mineralium Deposita*, v. 38, p. 968–983.
- WILKINSON, J.J., 2010, A review of fluid inclusion constraints on mineralization in the Irish ore field and implication for the genesis of sediment-hosted Zn-Pb deposits: *Economic Geology*, v. 105, p. 417–442.
- WILKINSON, J.J., AND EARLS, G., 2000, A high-temperature hydrothermal origin for black dolomite matrix breccias in the Irish Zn-Pb orefield: *Mineralogical Magazine*, v. 64, p. 1017–1036.
- WILKINSON, J.J., EYRE, S.L., AND BOYCE, A.J., 2005, Ore-forming processes in Irish-type carbonate-hosted Zn-Pb deposits: evidence from mineralogy, chemistry and isotopic compositions of sulfides at Lisheen Mine: *Economic Geology*, v. 100, p. 63–86.
- WILKINSON, J.J., AND HITZMAN, M.W., 2015, The Irish Zn-Pb orefield: the view from 2014, in Archibald, S.M., and Piercey, S.J., eds., *Current Perspectives on Zinc Deposits*: Dublin, Irish Association for Economic Geology, p. 59–72.
- WILLIAMS, F.M., SHEPPARD, W.A., AND MCARDLE, P., 1986, Avoca Mine, County Wicklow: a review of geological and isotopic studies, in Andrew, C.J., Crowe, R.W.A., Finlay, S., Pennell, W.M., and Pyne, J.F., eds., *Geology and Genesis of Mineral Deposits in Ireland*: Dublin, Irish Association for Economic Geology, p. 49–69.
- WILSON, M.E.J., EVANS, M.J., OXTOBY, N.H., SATRIA NAS, D., DONNELLY, T., AND THIRLWALL, M., 2007, Reservoir quality, textural evolution, and origin of fault-associated dolomites: American Association of Petroleum Geologists, *Bulletin*, v. 91, p. 1247–1272.
- WORONICK, R.E., AND LAND, L.S., 1985, Late burial diagenesis, Lower Cretaceous Pearsall and Lower Glen Rose Formations, south Texas, in Schneidermann, N., and Harris, P.M., eds., *Carbonate Cements*: SEPM, Special Publication 36, p. 265–275.
- WRIGHT, W.R., 2001, Dolomitization, fluid flow and mineralization of the Lower Carboniferous rocks of the Irish Midlands and Dublin Basin regions [PhD thesis]: University College Dublin, 407 p.
- WRIGHT, W.R., JOHNSON, A.W., SHELTON, K.L., SOMERVILLE, I.D., AND GREGG, J.M., 2000, Fluid migration and rock interactions during dolomitisation of the Dinantian Irish Midlands and Dublin Basin: *Journal of Geochemical Exploration*, v. 69–70, p. 159–164.
- WRIGHT, W.R., SOMERVILLE, I.D., GREGG, J.M., SHELTON, K.L., AND JOHNSON, A.W., 2001, Application of regional dolomite cement CL (cathodoluminescence) microstratigraphy to the genesis of Zn-Pb mineralization in lower Carboniferous rocks, Ireland: similarities to the southeast Missouri Pb-Zn district?, in Hagni, D., ed., *Studies on Ore Deposits, Mineral Economics, and Applied Mineralogy: With Emphasis on Mississippi Valley-Type Base Metal and Carbonate-Related Ore Deposits*: University of Missouri–Rolla Press, p. 1–17.
- WRIGHT, W.R., SOMERVILLE, I.D., GREGG, J.M., JOHNSON, A.W., AND SHELTON, K.L., 2003, Dolomitization and neomorphism of Irish Lower Carboniferous (Early Mississippian) limestones: evidence from petrographic and isotopic data, in Ahr, W., Harris, A.P., Morgan, W.A., and Somerville, I.D., eds., *Permo-Carboniferous Carbonate Platforms and Reefs*: SEPM, Special Publication 78 and American Association of Petroleum Geologists, *Memoir* 83, p. 395–408.
- WRIGHT, W.R., SOMERVILLE, I.D., GREGG, J.M., SHELTON, K.L., AND JOHNSON, A.W., 2004, Irish Lower Carboniferous replacement dolomite: isotopic modeling evidence for a diagenetic origin involving low-temperature modified seawater, in Braithwaite, C., Rizzi, G., and Darke, G., eds., *The Geometry and Petrogenesis of Dolomite Hydrocarbon Reservoirs*: Geological Society of London, Special Publication 235, p. 75–97.
- ZHANG, Y.G., AND FRANTZ, J.D., 1989, Experimental determination of the compositional limits of immiscibility in the system  $\text{CaCl}_2\text{-H}_2\text{O-CO}_2$  at high temperatures and pressures using synthetic fluid inclusions: *Chemical Geology*, v. 74, p. 289–308.

Received 26 February 2018; accepted 28 February 2019.